ผลของโปรโมเตอร์ต่อสมบัติของตัวเร่งปฏิกิริยานิกเกิลบนอะลูมินาที่เตรียมโดยปฏิกิริยาในภาวะ
ของแข็ง

นางสาวฐิติพร แซ่ลิ้ม

วิทยานิพนธ์นี้เป็นส่วนหนึ่งของการศึกษาตามหลักสูตรปริญญาวิศวกรรมศาสตรมหาบัณฑิต
สาขาวิชาวิศวกรรมเคมี ภาควิชาวิศวกรรมเคมี
คณะวิศวกรรมศาสตร์ จุฬาลงกรณ์มหาวิทยาลัย
ปีการศึกษา 2556
ลิขสิทธิ์ของจุฬาลงกรณ์มหาวิทยาลัย

THE EFFECT OF PROMOTERS ON THE PROPERTIES OF NI/AL2O3 CATALYSTS

PREPARED BY SOLID STATE REACTION

Miss Titiporn Sae-lim

A Thesis Submitted in Partial Fulfillment of the Requirements

for the Degree of Master of Engineering Program in Chemical Engineering

Department of Chemical Engineering

Faculty of Engineering

Chulalongkorn University

Academic Year 2013

Thesis Title                        THE EFFECT OF PROMOTERS ON THE PROPERTIES OF NI/AL2O3 CATALYSTS PREPARED BY SOLID STATE REACTION

By                              Miss Titiporn Sae-lim

Field of Study                 Chemical Engineering

Thesis Advisor                Associate Professor Joongjai Panpranot, Ph.D.

Accepted by the Faculty of Engineering, Chulalongkorn University in Partial Fulfillment of the Requirements for the Master's Degree

........................................................Dean of the Faculty of Engineering

(Professor Bundhit Euaarporn, Ph.D.)

THESIS COMMITTEE

........................................................Chairman

(Associate Professor Bunjerd Jongsomjit, Ph.D.)

........................................................Thesis Advisor

(Associate Professor Joongjai Panpranot, Ph.D.)

........................................................Examiner

(Chutimon Satirapipathkul, D.Eng.)

........................................................External Examiner

(Assistant Professor Okorn Mekasuwandumrong, D.Eng.)

iv

ฐิติพร แซ่ลิ้ม : ผลของโปรโมเตอร์ต่อสมบัติของตัวเร่งปฏิกิริยานิกเกิลบนอะลูมินาที่
เตรียมโดยปฏิกิริยาในภาวะของแข็ง. (THE EFFECT OF PROMOTERS ON THE
PROPERTIES OF NI/AL2O3 CATALYSTS PREPARED BY SOLID STATE
REACTION) อ.ที่ปรึกษาวิทยานิพนธ์หลัก: รศ. ดร. จูงใจ  ปั้นประณต, 82 หน้า.

ในงานวิจัยนี้ได้ทำการศึกษาผลของโปรโมเตอร์ที่ส่งผลต่อสมบัติของตัวเร่งปฏิกิริยา
นิกเกิลบนอะลูมินาที่เตรียมจากปฏิกิริยาในภาวะของแข็งระหว่างกิบบ์ไซต์ นิกเกิลไนเตรต และ
โปรโมเตอร์ชนิดต่างๆ ได้แก่ แมงกานีสอะซิเตต และคอปเปอร์ไนเตรต โดยการเผาในอากาศที่
อุณหภูมิ 500 องศาเซลเซียส เป็นเวลา 3 ชั่วโมง ทดสอบความสามารถของตัวเร่งปฏิกิริยาในการ
ทำปฏิกิริยาไฮโดรจิเนชันของคาร์บอนไดออกไซด์ ที่อุณหภูมิ 500  องศาเซลเซียส ความดัน
บรรยากาศ พบว่าตัวเร่งปฏิกิริยาที่ทำการปรับปรุงด้วยแมงกานีสให้ค่าความว่องไวสูงสุดใน
ปฏิกิริยาไฮโดรจิเนชันของคาร์บอนไดออกไซด์ เนื่องจากการแพร่กระจายของโลหะนิกเกิลบน
พื้นผิวของอะลูมินาที่สูงและอุณหภูมิในการรีดิวซ์ตัวเร่งปฏิกิริยาที่ต่ำลงส่งผลให้เกิดการรีดิวซ์เป็น
โลหะนิกเกิลได้ง่ายขึ้น นอกจากนี้การเพิ่มปริมาณของแมงกานีสและนิกเกิลบนตัวเร่งปฏิกิริยายัง
ช่วยเพิ่มความสามารถในการทำปฏิกิริยาได้สูงขึ้นเมื่อเปรียบเทียบตัวเร่งปฏิกิริยานิกเกิลที่ยังไม่ได้
ทำการปรับปรุงพบว่าตัวเร่งปฏิกิริยาที่เตรียมโดยวิธีการเคลือบฝังแบบเปียกให้ค่าความว่องไวใน
การทำปฏิกิริยาสูงกว่าที่เตรียมโดยปฏิกิริยาในภาวะของแข็ง อย่างไรก็ตามเมื่อทำการปรับปรุง
ตัวเร่งปฏิกิริยานิกเกิลด้วยแมงกานีสพบว่าตัวเร่งปฏิกิริยาที่เตรียมโดยปฏิกิริยาในภาวะของแข็งให้
ค่าความว่องไวในการทำปฏิกิริยาสูงกว่าที่เตรียมโดยวิธีการเคลือบฝังแบบเปียกโดยช่วยปรับปรุง
การกระจายตัวของโลหะนิกเกิลและความสามารถในการรีดักชัน

| | | | |
|---|---|---|---|
| ภาควิชา | วิศวกรรมเคมี | ลายมือชื่อนิสิต | |
| สาขาวิชา | วิศวกรรมเคมี | ลายมือชื่อ อ.ที่ปรึกษาวิทยานิพนธ์หลัก | |
| ปีการศึกษา | 2556 | | |

# # 5570176121 : MAJOR CHEMICAL ENGINEERING

KEYWORDS: NICKEL CATALYST / PROMOTER / SOLID-STATE REACTION / CARBON DIOXIDE HYDROGENATION

TITIPORN SAE-LIM: THE EFFECT OF PROMOTERS ON THE PROPERTIES OF NI/AL2O3 CATALYSTS PREPARED BY SOLID STATE REACTION. ADVISOR: ASSOC. PROF. JOONGJAI PANPRANOT, Ph.D., 82 pp.

In this research, the effect of Mn and Cu promoters on the properties of Ni/Al2O3 catalysts prepared by the solid-state reaction of gibbsite, nickel nitrate, and promoters at 500℃ for 3 h has been studied. The catalytic performances were tested in the carbon dioxide hydrogenation at 500℃ and atmospheric pressure. It was found that the modified nickel catalysts with Mn exhibited the highest $CO_2$ conversion in $CO_2$ hydrogenation. The superior catalytic performance can be explained by higher Ni dispersion and a lower reduction temperature so that the reduction of NiO was easier. Further increasing the amounts of manganese and nickel on the catalysts also improved the catalytic activity. Comparing the non-modified Ni catalysts, the catalysts prepared by incipient wetness impregnation exhibited higher $CO_2$ conversion than the ones prepared by the solid-state reaction. However, when modified with Mn the modified Ni catalysts obtained from the solid-state reaction exhibited higher $CO_2$ conversion than the incipient wetness impregnation due to improved Ni dispersion and reducibility.

| | | | |
|---|---|---|---|
| Department: | Chemical Engineering | Student's Signature | .......................... |
| Field of Study: | Chemical Engineering | Advisor's Signature | .......................... |
| Academic Year: | 2013 | | |

## ACKNOWLEDGEMENTS

# CONTENTS

# LIST OF TABLES

## LIST OF FIGURES

# CHAPTER 1

# INTRODUCTION

## 1.1 Rationale



**Figure 1.**1  Carbon dioxide emission [1]**.**

Increasing energy supply during recent years has caused the increasing of carbon dioxide emissions. Besides, human activities has contributed to an increase concentration of carbon dioxide in the atmosphere such as the combustion of fossil fuels (principally natural gas and crude oil), electricity production, manufacturing industry, and clearing the forests. The greenhouse gases were ranked to influential the greenhouse effect [2]

| Compound | Formula | Contribution |
|---|---|---|
| water vapor and clouds | $H_2O$ | 36-72% |
| carbon dioxide | $CO_2$ | 9-26% |
| methane | $CH_4$ | 4-9% |
| ozone | $O_3$ | 3-7% |

Therefore, global warming that caused by carbon dioxide emission should be reduced. There are many investigations on the conversion of carbon dioxide into valuable chemical compounds such as methane, or higher hydrocarbons. The carbon dioxide hydrogenation is one of the reactions to convert carbon dioxide into linear hydrocarbons that has been studied recently.

Immense studies on carbon dioxide hydrogenation have employed various metal-based catalysts such as cobalt, nickel, iron, and ruthenium. Nickel-based catalysts are interesting because of their high catalytic activity, high methane selectivity, and relatively low cost compared to noble metal. In addition, nickel has high thermal stability which can be used in a large range of reaction conditions. However, nickel catalysts usually produce high carbon deposition, resulting in catalyst deactivation and plugging in the reactor. Addition of a second metal promoter has shown to improve the properties of nickel-based catalyst in carbon dioxide hydrogenation. For example, Zheo et al. (2012) reported that the composite of Ni-Mn catalysts prepared by a co-impregnation method improved their catalytic activity. The manganese addition showed higher methanation activity and improved the surface area of catalysts and average pore volume. The impregnation method is the most extensive used method for catalyst preparation, however, several steps including drying and calcination are necessary. The solid-state reaction is direct reaction of mixture of materials. The advantages of this method are that it is simpler, cheaper, and gives high yields of products [3].

In the present work, the effects of various promoters on the properties of $Ni/Al_2O_3$ catalyst prepared by the solid-state reaction were investigated in the carbon dioxide hydrogenation. For comparison purposes, the conventional impregnation method was also employed for preparation of the Ni-based catalysts. The catalysts were characterized by X-ray diffraction (XRD), hydrogen temperature program reduction ($H_2$-TPR), nitrogen physisorption, scanning electron microscope analyses (SEM), X-ray photoelectron spectroscopy (XPS), and $H_2$ chemisorption. And the catalytic activities of $Ni/Al_2O_3$ catalysts were studied in the carbon dioxide hydrogenation.

## 1.2 Objective

The objective of this study is to investigate the effects of promoters on the properties of $Ni/Al_2O_3$ catalysts prepared by the solid- state reaction between gibbsite, nickel precursor and the promoters in the $CO_2$ hydrogenation.

## 1.3 Research Scopes

1.3.1    Study about the relating research and summary toward the interesting literature reviews.

1.3.2    Preparation the Ni-based catalysts with promoters by solid-state reaction using the mixture of nickel nitrate, gibbsite, and different promoters and calcined at 500°C.

1.3.3    Preparation the $Ni/Al_2O_3$ catalysts by incipient wetness impregnation using calcination of gibbsite at $500^{\circ}C$ and then impregnated with a mixture of aqueous solution of nickel nitrate and the promoter.

1.3.4    Performance of the catalytic activity for the carbon dioxide hydrogenation of $Ni/Al_2O_3$ catalysts at reaction temperature 500°C and 1 atm total pressure.

1.3.5    Characterization of $Ni/Al_2O_3$ catalysts using X-ray diffraction (XRD), Nitrogen physisorption, Hydrogen temperature program reduction ($H_2$-TPR), Scanning electron microscope analyses (SEM), X-ray photoelectron spectroscopy (XPS), and $H_2$ chemisorption.

## 1.4 Research Methodology

### 1.4.1 Part 1: Effect of Mn and Cu modification on the Ni/Al$_2$O$_3$ catalysts

```
┌─────────────────────────────────────────┐
│      Study about the relating research    │
└─────────────────────────────────────────┘
                    │
                    ▼
┌─────────────────────────────────────────────────────┐
│  Preparation the Ni-based catalysts with promoters by │
│  solid-state reaction using the 20 wt% Ni/Al₂O₃       │
│  catalysts with 1 wt% Mn and Cu                        │
└─────────────────────────────────────────────────────┘
                    │
                    ▼
┌─────────────────────────────────────────────────────┐
│  Preparation the Ni/Al₂O₃ catalysts by incipient      │
│  wetness impregnation using calcination of gibbsite    │
│  at 500°C                                              │
└─────────────────────────────────────────────────────┘
                    │
                    ▼
┌─────────────────────────────────────────────────────┐
│  Study in carbon dioxide hydrogenation reaction        │
└─────────────────────────────────────────────────────┘
                    │
                    ▼
┌─────────────────────────────────┐         ┌──────────────────────┐
│  Characterization of catalysts    │────────▶│  • XRD               │
└─────────────────────────────────┘         │  • N₂-physisorption   │
                    │                         │  • H₂-TPR            │
                    ▼                         │  • SEM               │
┌─────────────────────────────────┐         │  • XPS               │
│           Discussion             │         │  • H₂ chemisorption  │
└─────────────────────────────────┘         └──────────────────────┘
```

- Preparation the Ni-based catalysts with promoters by solid-state reaction using the 20 wt% Ni/Al$_2$O$_3$ catalysts with 1 wt% Mn and Cu
- Preparation the Ni/Al$_2$O$_3$ catalysts by incipient wetness impregnation using calcination of gibbsite at 500$^\circ$C
- Study in carbon dioxide hydrogenation reaction
- Characterization of catalysts
  - XRD
  - N$_2$-physisorption
  - H$_2$-TPR
  - SEM
  - XPS
  - H$_2$ chemisorption
- Discussion

**1.4.2 Part 2: Effect of the amounts of Mn promoters**

Study about the relating research

↓

Preparation the Ni/Al$_2$O$_3$ catalysts with the best promoter by solid-state reaction using the 20 wt% Ni/Al$_2$O$_3$ catalysts with 0, 0.25, 0.5, 1, 2wt% promoter

↓

Study in carbon dioxide hydrogenation reaction

↓

Characterization of catalysts  →  

- XRD
- N$_2$-physisorption
- H$_2$-TPR
- SEM
- XPS
- H$_2$ chemisorption

↓

Discussion
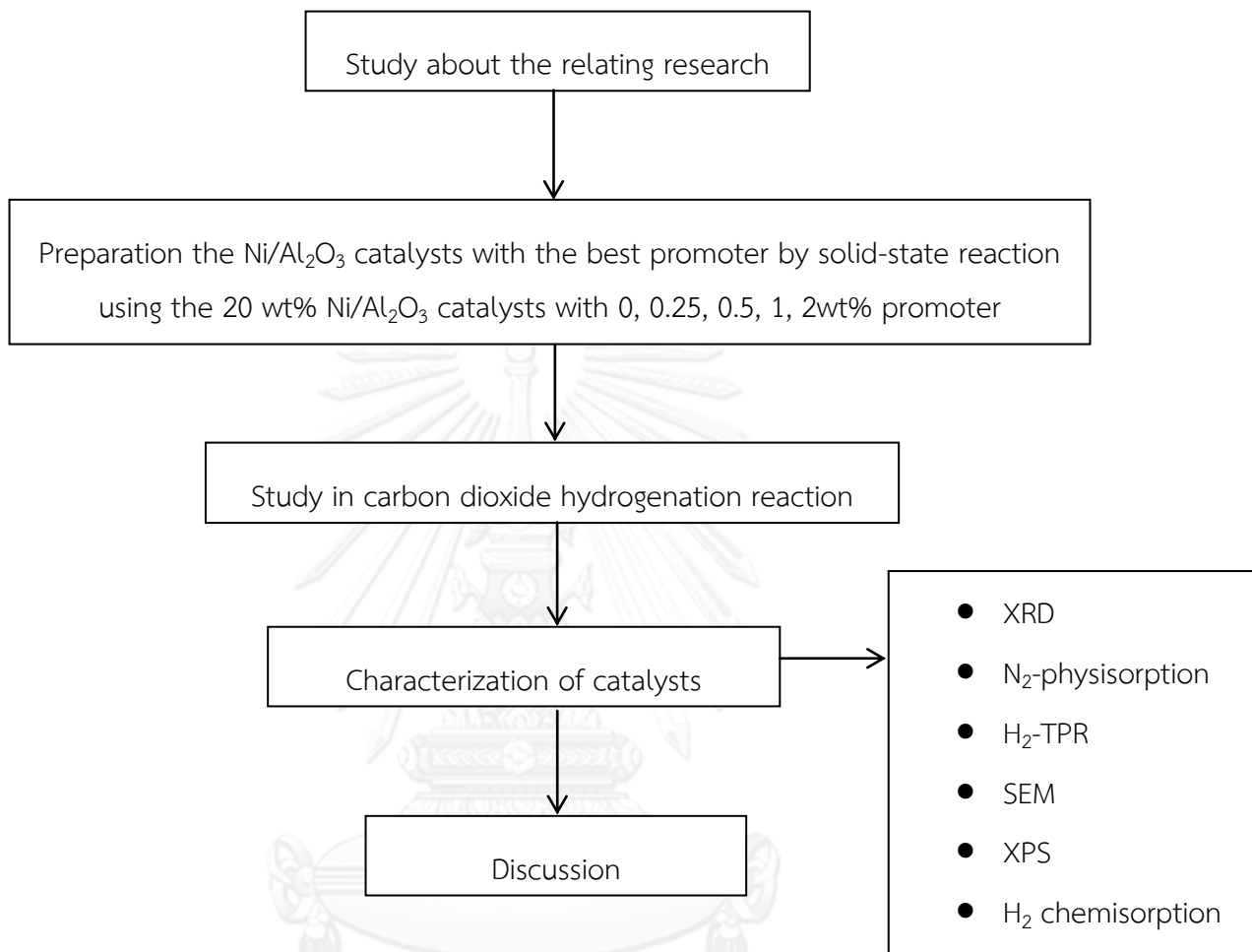
### 1.4.3 Part 3: Effect of the amounts of nickel

```
┌─────────────────────────────────────────┐
│      Study about the relating research    │
└─────────────────────────────────────────┘
                    │
                    ▼
┌───────────────────────────────────────────────────────────┐
│ Preparation the Ni/Al₂O₃ catalysts with the best promoter by solid-state │
│ reaction using the best amount of promoter with the 5, 10, 15, 20 wt% nickel │
└───────────────────────────────────────────────────────────┘
                    │
                    ▼
┌───────────────────────────────────────────────┐
│ Study in carbon dioxide hydrogenation reaction │
└───────────────────────────────────────────────┘
                    │
                    ▼
┌─────────────────────────────┐
│ Characterization of catalysts │──────►
└─────────────────────────────┘
                    │
                    ▼
┌─────────────────┐
│    Discussion    │
└─────────────────┘
```

Preparation the Ni/Al$_2$O$_3$ catalysts with the best promoter by solid-state reaction using the best amount of promoter with the 5, 10, 15, 20 wt% nickel

Study in carbon dioxide hydrogenation reaction

Characterization of catalysts

- XRD
- N$_2$-physisorption
- H$_2$-TPR
- SEM
- XPS
- H$_2$ chemisorption

Discussion

**1.4.4 Part 4: Effect of the preparation methods between solid-state reaction and incipient wetness impregnation**

```
┌─────────────────────────────────────────┐
│      Study about the relating research   │
└─────────────────────────────────────────┘
                    │
                    ▼
┌─────────────────────────────────────────────────────────────────────┐
│  Preparation the Ni/Al₂O₃ catalysts by solid-state reaction and       │
│  incipient wetness impregnation using the 5 and 20 wt% Ni catalysts   │
│  with 0 and 0.5 wt% Mn  promoter                                       │
└─────────────────────────────────────────────────────────────────────┘
                    │
                    ▼
┌─────────────────────────────────────────────────────┐
│   Study in carbon dioxide hydrogenation reaction      │
└─────────────────────────────────────────────────────┘
                    │
                    ▼
          ┌─────────────────────────────┐
          │          Discussion          │
          └─────────────────────────────┘
```

Preparation the $Ni/Al_2O_3$ catalysts by solid-state reaction and incipient wetness impregnation using the 5 and 20 wt% Ni catalysts with 0 and 0.5 wt% Mn promoter

CHAPTER 2

THEORY

In this chapter, relating research and theory regarding carbon dioxide hydrogenation reaction, solid state reaction, alumina, and nickel are presented.

## 2.1  Carbon dioxide hydrogenation reaction

Carbon dioxide as carbon-containing resources leading to a greenhouse gas that needs to be reduced. Therefore, attempts have been developed the technology is applied for carbon dioxide capture and recycling. Recycling of carbon dioxide for in the production of fuels or other chemicals[4]. Carbon dioxide is released as a co-reactant for the methanol and alcohols synthesis or a by-product of the Fischer-Tropsch synthesis (FTS). Carbon dioxide hydrogenation reaction is different from the Fischer-Tropsch reaction, wherewith its lower deactivation rates. Many catalysis processes are used to derive synthesis products from carbon dioxide.
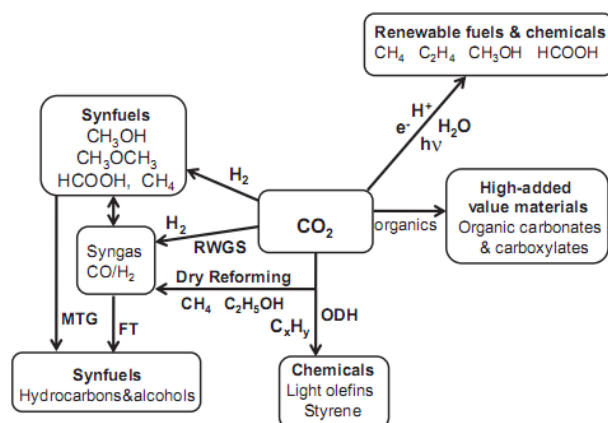


Figure 2.1 Catalytic routes for carbon dioxide activation
in heterogeneous phase[5]

The catalytic reaction for using carbon dioxide in the synthesis of hydrocarbons and alcohols products called the Sabatier reaction.

$$CO_2(g) + 4H_2(g) \longrightarrow CH_4(g) + 2H_2O(g) \qquad (2.1)$$
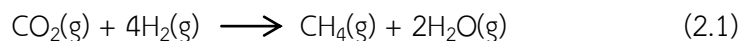
The hydrogenation of $CO_2$ is exothermic, anywise, this reaction requires an eight electrons for reduction of carbon dioxide into methane which leading to kinetic limitations which use a catalyst to achieve desirable rates and selectivity. Two main mechanisms are synthesized for the methanation of $CO_2$. Firstly, the formation of CO and then its posterior conversion to methane. The intermediates are the adsorbed formyl species $(HCO)_{ads}$ or surface carbon $(C_{ads})$ and then theirs hydrogenated to produce methane. Secondary, $CO_2$ is directly hydrogenated without intermediate CO formation. The hydrogen carbonate $(HCO3)_{ads}$ and formate $(HCOO)_{ads}$ surface species are used aspossible intermediates. The hydrogenation of intermediates adsorbed on the metal-support interface which, its as the key step in the formation of methane.
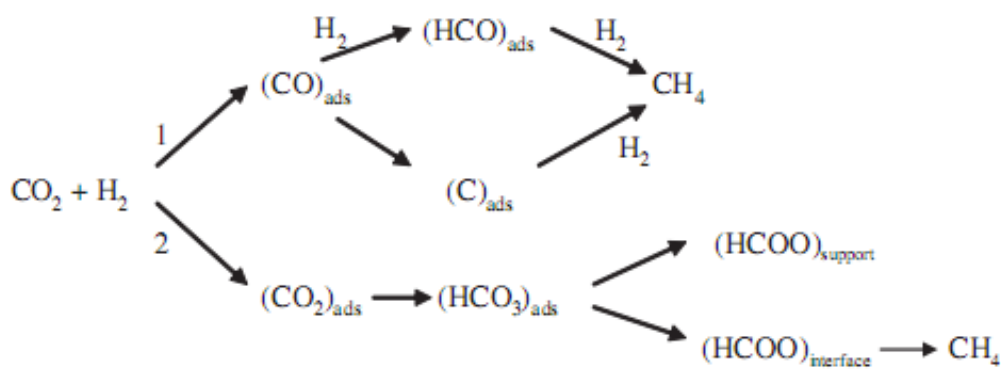


Figure 2.2 The pathways of carbon dioxide methanation on supported metal catalysts [5]

## 2.2 Solid state reaction

Several methods can be used to synthesize solids. The solids are prepared by a different routes, particularly these are not thermodynamically stable leading to be difficult to prepare. Solid state reaction is how to prepare the single phase compounds. This synthesis method is the oldest, simplest, and most widely used to mix together powder reactants sometimes compress them into pellets or other shape then calcination for a long time. This method is internally slow because the reactants are very inhomogeneous in the atomic level albeit they may be well-mixed at the level of individual particles. The immense amount of mixing of atoms in particles is required. The solid state or liquid or gas phase transport bring together atoms of the variant elements to form the desired product. [6]

Classification of the reactions leading to the formation of homogeneous solid phase based on the physical state of the reactants and the products as shown :

$$Type\ I \qquad A(s) \qquad \longrightarrow \qquad B(s) + C(g) \qquad (2.2)$$

$$Type\ II \qquad A(s) + B(s) \qquad \longrightarrow \qquad C(s) \qquad (2.3)$$

$$Type\ III \qquad A(s) + B(s) \qquad \longrightarrow \qquad C(s) + D(g) \qquad (2.4)$$

$$Type\ IV \qquad A(s) + B(g) \qquad \longrightarrow \qquad C(s) \qquad (2.5)$$

$$Type\ V \qquad A(s) + B(g) \qquad \longrightarrow \qquad C(s) + D(g) \qquad (2.6)$$

$$Type\ VI \qquad A(s) \qquad \longrightarrow \qquad B(g) + C(g) \qquad (2.7)$$
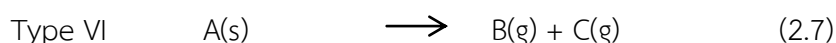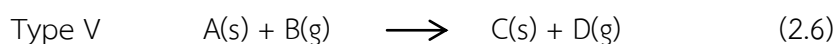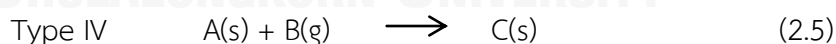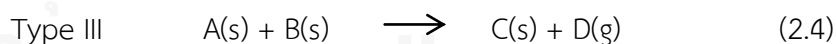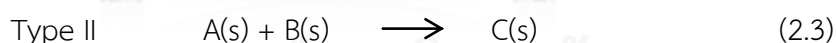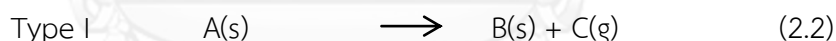
The type I reactions may be either endothermic or exothermic, mostly studied about endothermic reactions is the dehydration of the metal salt hydrate and the

decomposition of the metal carbonates. The decomposition product of the metal hydrates has a crystal lattice solid or crystal structure. The dehydration of the crystalline hydrate forms are greatly unregulated product, which bring about to new crystalline phase. The example of the decomposition of calcium carbonate is

$$CaCO_3(s) \longrightarrow CaO(s) + CO_2(g) \qquad (2.8)$$
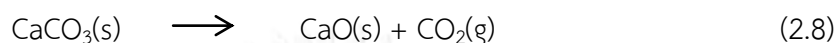
The type II reactions about two solid phases, which the atoms have finite movement. The reaction will be built up only at the points of contact of two phases and a product layer. The reaction depends on the diffusion of reactants over the product layer and the rate of reaction depends on the transfer rate of atoms or ions over the product layer. Therefore, the structure of the product phase B is effected to the reaction. The diffusion path can be abridged by using the fine particles of the reactants so, the new form phase is poorly crystalline and a high concentration of defects. The example of the type II reaction  such as

$$ZnO(s) + Al_2O_3(s) \longrightarrow ZnAl_2O_4(s) \qquad (2.9)$$

The reactivity of solids are improved so that the product can be built up in a shorter time and under conditions. The method can be created in many ways as shown [7]:

- Increasing the surface area of the reactant
- Preparation of compounds over single phase precursor
- Addition of impurities in solid during crystallization
- The structure of a solid effects
- The coupling effect bring about to a new form solid
- The effect of high energy radiations

## 2.3  Alumina

Alumina has high melting point (over 2000°C) which is used to desirable for the support. Wherewith, it has the high melting point, so it has immense characteristics for separating particles of a catalytic substance from each other and as a support as a catalyst thermal stabilizer. The alumina will be prevented from agglomerating or coalescing.

The characteristic of alumina is transition phases that over a very catholic temperature range. There are six principal phases defined by the Greek letters included that chi, kappa, eta, theta, delta, and gamma. The nature of the product received by calcination depending on the starting matter such as gibbsite, boehmite, and others.

The field of structures of aluminas are classified to three classes:

2.3.1   Aluminum trihydroxides (Al(OH)$_3$)

2.3.2   Aluminum oxyhydroxides (AlO(OH))

2.3.3   Aluminum oxides (It is distinguished between transition aluminas and alpha alumina)

### Aluminum Trihydroxides

Three crystallized forms that the formula Al(OH)$_3$consist of Gibbsite, Bayerite, and Nordstrandite. The Gibbsite is the major part calcined to corundum for the manufacture of aluminum. The crystallized trihydroxides may be brought about to amorphous hydroxide synthesis under condition of pH and temperature.

### Aluminum Oxyhydroxide

The formula AlO(OH).xH$_2$O consist of boehmite, and diaspora. It is useful to divide a third form, called pseudoboehmite or microcrystalline boehmite, which is derived from boehmite but with specific properties. [8]
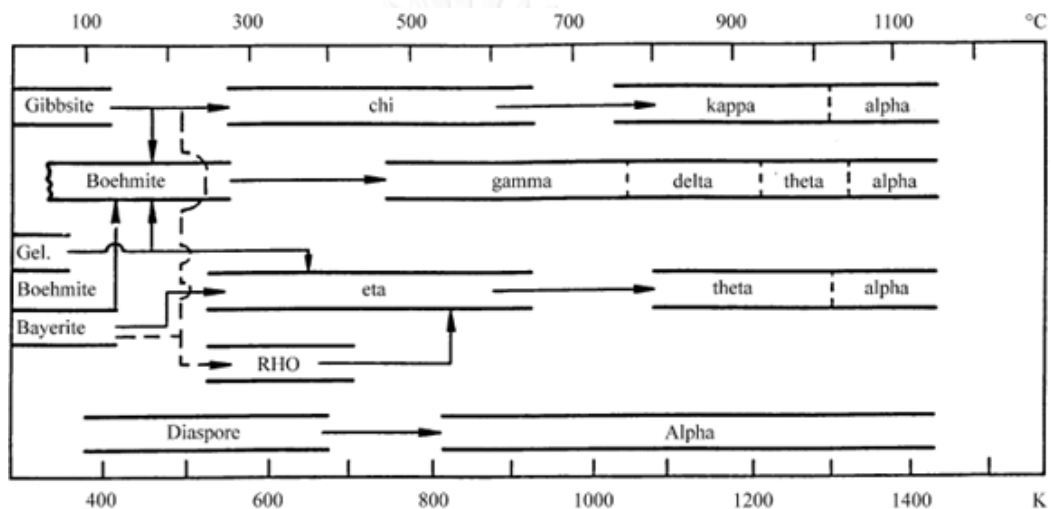


Figure 2.3  Decomposition sequence of aluminum hydroxides [9]

## 2.4  Nickel

Nickel, the transition metals having atomic number 28 and chemical symbol Ni. Powder nickel has maximum surface area on which reactions but the larger metal are long to react in air at ambient conditions so they are considered corrosion-resistant. A compound of nickel is used in chemical manufacturing such as a catalyst for hydrogenation.

Nickel is the transition metals, which has two electronic configurations that is [Ar] $4s^2$ $3d^8$ and [Ar] $4s^1$ $3d^9$. The crystalline structure of nickel is a face centered

cube (FCC) and the lattice parameter of 0.352 nm having an atomic radius of 0.124 nm.

Nickel has +2 valance states for the major common oxidation state. but nickel compounds have three well known such as $Ni^0$, $Ni^+$, and $Ni^{3+}$ and exotic oxidation states such as $Ni^{2-}$, $Ni^{1-}$, and $Ni^4$.

Nickel (0) is a volatile, which is highly toxic liquid at ambient temperature when its heated, the compound disintegrates to nickel and carbon monoxide.

$$Ni(CO)_4 \rightleftharpoons Ni + 4CO \qquad\qquad (2.10)$$

Nickel (I) compounds are uncommon, for example the tetrahedral complex $NiBr(PPh_3)_3$. This complex is oxidized in water.

Nickel (II) complexes are common anions, such as the sulfide, sulfate, carbonate, hydroxide, carboxylates, and halides. The nickel salts (chloride, nitrate, and sulfate) can dissolve in water and provide green solutions (metal aquo complex $[Ni(H_2O)_6]^{2+}$). The tetracoordinate nickel (II) compounds consist of tetrahedral and square planar geometries. The tetrahedral compounds are paramagnetic but the square planar compounds are diamagnetic.

Nickel (III) and nickel (IV) transpires with fluoride and oxides. Nickel (III) is nickel (III) oxide but nickel (IV) is the mixed oxide $BaNiO_3$ that its employed the cathode in rechargeable batteries. The $\sigma$-donor ligands (thiols and phosphines) can stabilize nickel (III) [10].

CHAPTER 3

LITERATURE REVIEW

This chapter summarizes the scientific research, which relates to the concerned research. These reviews are divided into two groups. In the first section, it describes the effects of promoters on the properties of $Ni/Al_2O_3$ catalysts in methanation reaction and $CO_2$ hydrogenation. In the second section, it shows the effects of different catalysts in CO and $CO_2$ hydrogenation.

## 3.1 The effects of promoters on the properties of $Ni/Al_2O_3$ catalysts in methanation reaction and $CO_2$ hydrogenation

Zhao et al. (2012) investigated the effect of manganese loading contents (1-3 wt%) promoter on the catalytic properties of $Ni/Al_2O_3$ catalysts for the syngas methanation reaction. The catalysts were prepared by co-impregnation method. It was found that the addition of Mn exhibited higher syngas methanation activity and stability wherewith the manganese can improve the average pore volume and surface area. The XRD patterns corresponding to manganese oxides crystalline phase were not detected. The manganese oxides were formed small particles so, the high dispersion on the surface of catalysts. The TPR profiles of catalysts were found that the addition of 1 wt% Mn exalted the reducibility of nickel oxides and formatted the small nickel particles which increased the activity and stability at high temperatures. While the addition of 3 wt% Mn formatted the large nickel particles which actived at low temperatures. [11]

Liu et al. (2012) synthesized the methanation of carbon dioxide with hydrogen using the $Ni-CeO_2/Al_2O_3$ catalysts. The catalysts were prepared by impregnation

boehmite. They studied the effects of cerium oxide loading content 0-6 wt%. The catalytic activity showed that depend on the cerium oxide loading. The sample with 2 wt% cerium oxide was found to the highest activity at reaction temperature 350°C and stability of 120 h when comparing non-modified $CeO_2$ catalysts. The $CeO_2$ can improve reducibility of the catalysts was decreased the reduction temperature towards lower temperature.[4]

Liu et al. (1999) studied the carbon dioxide hydrogenation activity of the bimetallic Cu-Ni/$Al_2O_3$ catalysts. The catalysts were produced by the co-impregnation method containing the different ratio of Cu:Ni at 773 K and 873 K at atmospheric pressure with a GHSV of 2,000/h. The catalysts contain the loading Cu/Ni in the ratio 3:1, 1:1, 1:3, and 1:5 (20% total metal content). It found that the ratio of Cu/Ni = 3:1 has the highest carbon dioxide conversion and carbon monoxide selectivity at 773 K and 873 K. This results suggested that the increase of copper can improve adsorption of the amount of carbon dioxide, it brings about to carbon monoxide production while nickel goes to be methane formation. The nickel is of benefit to hydrogen adsorption. Moreover, the catalytic performance of the bimetallic catalysts had higher at reaction temperature 873 K (28.7% $CO_2$ conversion).[12]

## 3.2 The effects of different catalysts in the carbon monoxide and carbon dioxide hydrogenation

Dorner et al. (2011) reported the use of bifunctional catalyst for $CO_2$ hydrogenation. The catalysts can combine both reverse water-gas-shift and Fischer-Tropsch synthesis on the ceria modified Fe/Mn/K catalysts. Moreover, they studied the effect of calcination temperature for catalytic properties at 500°C and 800°C. All catalysts were prepared by an incipient wetness impregnation method. It was found that the catalysts promoted with ceria showed 22% increase in carbon dioxide

conversion (41.4% to 50.4%). The ceria particles have lattice oxygen vacancies, which can oxidize the metal surface during the CO reaction. For the reaction temperature, the catalysts were calcined at 800°C which showed that increasing in $CO_2$ conversion and a 5% increase olefin/paraffin ratio. The ceria particles calcined at 800°C are larger in size than the ceria calcined at 500°C. Therefore, the catalyst has a larger concentration of ceria surface species. The metals on the top of the ceria were reduced for the active sites in reverse water-gas-shift. [13]

Srisawat et al. (2007) investigated the effect of amounts of alumina for cobalt catalysts dispersed on alumina-silica supports. The catalysts were characterized by XRD, TEM, TPR, SEM/EDX, $N_2$physisorption, and $H_2$ chemisorption. They were reported that the content of alumina exhibited the size of cobalt oxide. The high $Al_2O_3$ on alumina-silica bimodal supports which showed high activity because the reducibility of the catalysts was increased. Furthermore, the type of cobalt precursors involved the catalytic performance. The incipient wetness impregnation of alumina-silica and cobalt nitrate resulted the highest activity while the cobalt chloride resulted the lowest activity wherewith the dispersion of cobalt was decreased. [14]

Chitpong et al. (2007) studied of cobalt on zirconia supports promoted with boron. They were prepared the catalysts having boron loading contents 0.5-3 wt%. The result that the catalysts promoted with B showed increase the catalytic activity in carbon monoxide hydrogenation. The promotion with boron can prevent the glomerate cobalt oxide, and increase the spreading of cobalt oxide bring about to the reducibility of the cobalt oxide. Further, they were prepared the 1 wt% boron modified zirconia supports having cobalt loading contents 5-20 wt%. The catalysts were decreased the cobalt contents leading to decreasing the activity but increasing in $C_2$-$C_4$ selectivity. [15]

Chul Lee et al. (2004) reported the effect of a ruthenium component on Fe-K/γ-Al$_2$O$_3$ catalysts for carbon dioxide hydrogenation. The catalysts contain the compositions ratio of Fe:K:Al$_2$O$_3$ = 1.00:0.35:5.00 and Fe:Ru:K:Al$_2$O$_3$ = 1.00:0.05:0.35:5.00. All catalysts were investigated by BET, XRD, and temperature-programmed desorption of CO$_2$, CO and C$_2$H$_4$. The results reported that promotion with ruthenium can improve carbon dioxide conversion (36% to 41%). Comparing the non-modified iron-based catalysts, which showed higher methane (16 mol%) and the product selectivity of C$_2$-C$_4$ (39.6 mol%) than the non-modified Fe catalysts. However, promotion with ruthenium acquired higher hydrocarbons. The behavior of a ruthenium component will be increased the readsorption of α-olefin leading to higher length of hydrocarbon products. [16]

Taochaiyaphum et al. (2004) reported the catalytic performance of zirconia supported cobalt catalysts by the glycothermal method for CO hydrogenation. They studied the glycol types (1,4-butanediol (BG) and 1,5-pentanediol (PeG)) and zirconia concentrations (20.5 and 29.5%) which be the cause of catalytic activity. All catalysts were forearmed by the glycothermal manner, which were obtained large surface area of zirconia. The TPR profiles showed the lower reduction temperature in the ZrO$_2$ prepared in 1,4-BG for cobalt catalyst, which exhibited the highest hydrogen chemisorption and initial carbon monoxide hydrogenation activity. Rather, these of 1,4-BG supported revealed decreased rapidly activity. Thus, they added the small amount of silica into zirconia support. It found that steady-state rates of the catalysts were also increased. Further, comparing the micron and nano-size of commercial zirconia from Aldrich, the catalyst prepared by commercial nano-size zirconia showed higher CO hydrogenation activity than the micron-size zirconia. Anywise, the catalyst prepared by the glycothermal method represented the highest activity. [17]

Srisawad et al. (2010) studied about the types of cobalt precursors that affected the catalytic performance of Co/Al$_2$O$_3$ catalyst. The catalysts were prepared by solid-state reaction with four different cobalt salts (cobalt nitrate, cobalt

acetylacetonate, cobalt acetate and cobalt chloride) with gibbsite calcined for 5 h in air at 650℃. The reaction temperature at 270℃ and atmospheric pressure. The results of $CO_2$ hydrogenation of the prepared $Co/Al_2O_3$ catalysts with cobalt nitrate by solid-state reaction showed the highest $CO_2$ conversion. Another, comparing the Co catalysts prepared by solid-state reaction of cobalt nitrate exhibited the higher $CO_2$ conversion than the Co catalysts prepared by incipient wetness impregnation. As the catalysts, prepared by solid-state reaction performances can be better dispersion of the Co particles on the surface of support. [18]

# CHAPTER 4

# EXPERIMENTAL

## 4.1 Chemicals

The chemicals used in this research are assigned as followed:

**Table 4.1 Chemicals used for synthesis of the catalysts**

| Chemical | Supplier |
|---|---|
| Fine gibbsite | Merck |
| Nickel (II) nitrate hexahydrate 98% | Fluka |
| Manganese (II) acetate tetrahydrate 99% | Aldrich |
| Copper (II) nitrate 99% | Ajax Finechem |

## 4.2 Materials preparation

### 4.2.1 Catalyst preparation by solid-state reaction

The solid-state catalysts were prepared using the mechanical mixture of nickel nitrate, gibbsite, and different promoters (manganese acetate and copper nitrate). Ni loading of 20 wt% were modified by 1 wt% promoter. Firstly, the amount of nickel nitrate, gibbsite, and difference promoters were mixed in an agate mortar. Then, the mixed materials were dried at 110°C for overnight. Lastly, the catalysts sample were calcined in a tube furnace in air (95 ml/min) at 500°C, heating rate of 10°C/min and hold on this temperature for 3 h.

### 4.2.2   Catalyst preparation by incipient wetness impregnation

For the impregnation method, the catalysts sample was used for the reference catalyst. The alumina ($Al_2O_3$) support was prepared by calcinations of gibbsite in a tube furnace in air at 500°C for 3 h and then impregnated with a mixture of aqueous solution of nickel nitrate and the promoter. After impregnation, the catalyst samples were dried at 110°C for overnight and calcined for 3 h in air flow at 500°C.

## 4.3 Catalysts characterization

### 4.3.1   X-ray diffraction

The bulk phase of catalysts were characterized by powder X-ray diffraction (XRD) patterns on SIEMENS D 5000 using CuK$_\alpha$ radiation with Ni filter in the 2$\theta$ scanning range of 10-90 degrees and a step size of 0.4°.

### 4.3.2   N$_2$ physisorption

Nitrogen adsorption-desorption isotherms were analyzed by BET apparatus for the multiple point method. Two feed lines for helium and nitrogen were obtained for BET surface area measurement. The sample cell and rod were produced from pyrex glass. The mixture gases will slip through the sample at the nitrogen relative of 0.3. Using 0.1 g catalysts sample will be filled in the sample cell. The sample was heated up to 150°C and hold at the same temperature for 3 h. Then, the sample was cooled down to room temperature to measured amount of nitrogen. Firstly, the sample will be adsorbed by liquid nitrogen. Nitrogen gas was adsorbed on the surface of sample unless equilibrium. Then, the nitrogen gas-adsorption sample was dipped into the water in order that desorbed the nitrogen gas out of the surface of

sample until the indicator line was in base line. For the calibration step, the nitrogen gas 1 ml was injected into the calibration port in the gas chromatograph for area measurement.

### 4.3.3 Temperature-programmed reduction

Hydrogen temperature-programmed reduction ($H_2$-TPR) measurements were obtained with a Micrometritics Chemisorb 2750 apparatus. Firstly, using 0.1 g catalyst sample used in a quartz U-tube reactor. After that, the catalysts will be heated up to 500°C in flowing nitrogen and held at this temperature for 0.5 h and then cooled down to room temperature. $H_2$-TPR was conducted with the carrier gas of 10% $H_2$ in Ar at a flow rate of 25 ml.min$^{-1}$. The amount of hydrogen consumption was used by a thermal conductivity detector (TCD).

### 4.3.4 Scanning electron microscopy analyses (SEM)

The morphology of the catalyst particles were determined by scanning electron microscopy technique using model of SEM : JEOL mode JSM-5800LV.

### 4.3.5 X-ray photoelectron spectroscopy (XPS)

The composition on the surface of catalysts were measured by X-ray photoelectron spectroscopy (XPS) on AMICUS spectrometer using a Mg K-$\alpha$ X-ray radiation at 15 kV and current of 12 mA. The pressure analysis chamber was less than $10^{-5}$ Pa.

### 4.3.6    Hydrogen chemisorption

Hydrogen chemisorption was characterized by using a Micrometritics Chemisorb 2750 and ASAP 2101CV.3.00 software in order to measure the dispersion of metal particles. First step, using 0.2 g catalyst sample was carried out in glass reactor. Then, the sample was reduced in $H_2$ at a flow rate of 50 mL•min$^{-1}$ and heated up  to  623 K with a heating rate at 10 °C•min$^{-1}$ and held at 3 h. Final step, the sample was cooled down to room temperature in a flowing $N_2$ at a flow rate of 30 mL•min$^{-1}$ in the gas chromatograph with thermal conductivity detector (TCD).

## 4.4 Reaction in carbon dioxide hydrogenation

### 4.4.1    Materials

In this the reaction, the $CO_2$ in $H_2$ feed stream was used to the reactant gas from Thai Industrial Gas Limited (TIG). The $CO_2$ hydrogenation reaction was operated using 0.1 g catalyst sample packed in the quartz microreactor. The $H_2/CO_2$ ratio of 10/1 with the total gas flow rate was 21.2 ml/min. The catalyst was heated from ambient temperature to 400°C and then reduced in situ in flowing $H_2$ for 4 h. Reaction was carried out at 1 atm total pressure and 500°C. Gas composition was analyzed by gas chromatograph equipped with TCD (Thermal conductivity detector).

### 4.4.2    Apparatus

The $CO_2$ hydrogenation system includes a reactor, an electrical furnace, a temperature controller, a gas controlling system, and a gas chromatography.

### 4.4.2.1 Reactor

The reactor was produced from a quartz tube. The 0.1 g catalyst sample was filled between quartz wool layers.

### 4.4.2.2 Electrical furnace

The reactor was supplied heat from the electrical furnace. The reactor was heated from ambient temperature to 800°C at 220 volt.

### 4.4.2.3 Temperature controller

This system included a thermocouple that it was connected with temperature controller model no. SS2425DZ to measure the reactor temperature. The temperature controller is changed within the range 0-800°C at 220 volt.

### 4.4.2.4 Gas controlling system

The reactant gas was adjusted by a pressure regulator. The metering valves were used to alter the gas flow rates and on-off valve.

### 4.4.2.5 Gas chromatography

Gas composition in the feed and product streams were analyzed by a Shimadzu GC8A (molecular sieve 5 Å) gas chromatograph equipped with TCD (Thermal conductivity detector). The operating conditions are exhibited in the Table 4.2.

### 4.4.3 The $CO_2$ hydrogenation procedures

The carbon dioxide hydrogenation reaction was performed using 0.1 g catalyst sample packed in the quartz microreactor. The total gas flow rate was 21.2 ml/min

of 8.8% $CO_2$ in $H_2$, and 50 ml/min of $H_2$ with the $H_2/CO_2$ ratio of 10/1. The catalyst was heated from ambient temperature to 400°C and then reduced in situ in flowing hydrogen for 4 h. After that, reaction was carried out at 500°C and 1 atm total pressure. Gas composition was analyzed by gas chromatograph equipped with TCD (Thermal conductivity detector) for separation of carbon dioxide ($CO_2$), carbon monoxide (CO), hydrogen ($H_2$), and methane ($CH_4$).

Table 4.2  The operating conditions for GC

| Gas Chromatograph | Shimadzu GC-8A |
|---|---|
| Detector | TCD |
| Column | Molecular sieve 5 Å |
| - Column material | SUS |
| - Length | 2 m |
| - Outer diameter | 4 mm |
| - Mesh range | 60/80 |
| - Maximum temperature | 350°C |
| Carrier gas | He (99.999%) |
| Carrier gas flow | 40 ml/min |
| Column gas | He (99.999%) |
| Column gas flow | 40 ml/min |
| Column temperature | |
| - initial (°C) | 70 |
| - final (°C) | 70 |
| Detector temperature (°C) | 100 |
| Injector temperature (°C) | 100 |
| Current (mA) | 80 |

CHAPTER 5

RESULTS AND DISCUSSION

This chapter is divided into four parts. Part (5.1) illustrates the effect of modified $Ni/Al_2O_3$ catalysts by Mn and Cu which prepared by solid-state reaction and incipient wetness impregnation. Part (5.2) illustrates the effect of amounts of promoters that prepared by solid-state reaction. Part (5.3) illustrates the effect of the amounts of nickel which prepared by solid-state reaction. Part (5.4) illustrates the effect of preparation methods between solid-state reaction and incipient wetness impregnation. The Ni-based catalysts were prepared with nickel nitrate, gibbsite and various promoters such as manganese acetate and copper nitrate by solid-state reaction and incipient wetness impregnation. The catalysts were characterized by XRD, BET, $H_2$-TPR, SEM, XPS, and $H_2$ chemisorption. The performance of the catalytic activity in the $CO_2$ hydrogenation of $Ni/Al_2O_3$ catalysts were explained in this part.

## 5.1 Effect of Mn and Cu modification on the $Ni/Al_2O_3$ catalysts

### 5.1.1 Catalysts characterization

The catalyst nomenclatures are as shown below:

**NA** is referred to the catalyst prepared by solid-state reaction which was a mixture of nickel nitrate and gibbsite.

**NA-Imp** is referred to the catalyst prepared by incipient wetness impregnation which was a mixture of nickel nitrate and gibbsite calcined at 500℃.

**Mn-NA** is referred to the catalyst prepared by solid-state reaction composed of a mixture of manganese acetate, nickel nitrate, and gibbsite.

**Cu-NA** is referred to the catalyst prepared by solid-state reaction composed of a mixture of copper nitrate, nickel nitrate, and gibbsite.

**Mn-NA-Imp** is referred to the catalyst prepared by incipient wetness impregnation composed of mixture of manganese acetate, nickel nitrate and gibbsite calcined at 500°C.

### 5.1.1.1 X-ray diffraction (XRD)

The XRD patterns of Ni/Al$_2$O$_3$ catalysts with different promoters calcined at 500°C in air which were prepared by the solid-state reaction using the mixture of nickel nitrate, gibbsite, and promoter, and the incipient wetness impregnation are shown in Figure 5.1. The scans were recorded in the 2$\theta$ range of 10-90$^\circ$. The XRD diffraction peaks of all the Ni-loaded catalysts exhibited at 2$\theta$ degrees 37.3$^\circ$, 43.3$^\circ$, 62.9$^\circ$, 75.3$^\circ$, 79.5$^\circ$, which corresponded to the NiO crystalline phase [11]. There was no significant difference between the catalysts prepared by the solid-state reaction and the incipient wetness impregnation. In terms of Mn and Cu species, the XRD peaks corresponding to manganese oxides and copper oxides crystalline phase were not detected. This suggests that the crystallite size of the manganese oxides and copper oxides may be smaller than the detection limit of the XRD due to the very low amount present [3]. However, the Ni/Al$_2$O$_3$ catalysts that were promoted by Mn can decrease the NiO crystallite size but Cu promoted resulted in an increase of the NiO crystallite size instead for the same preparation method. The average NiO crystallite sizes after calcination at 500°C are summarized in Table 5.1. The NiO crystallite sizes of Ni-based catalysts with different promoters were ranged between 14.9-24.2 nm. That is, the NiO crystallite sizes prepared by the solid-state reaction showed larger sizes than the incipient wetness impregnation.
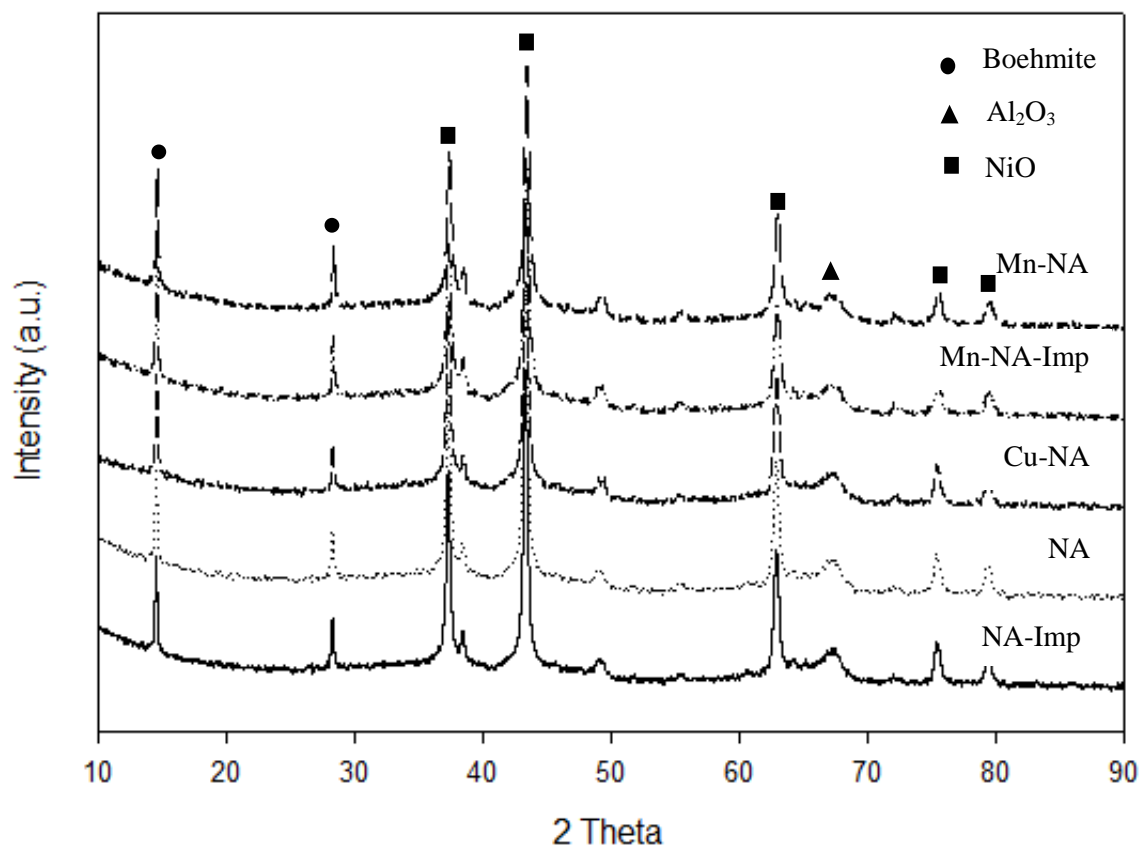
Figure 5.1 The XRD patterns of Ni/Al$_2$O$_3$ catalysts with different promoters,
● = Boehmite; ■= NiO;  ▲= Al$_2$O$_3$, NA-Imp (a), NA (b), Cu-NA (c), Mn-NA-Imp (d),
Mn-NA (e).

Table 5.1 Average NiO crystallite size of unmodified and modified with manganese and copper promoters of nickel catalysts

| Sample | Average NiO crystallite size from XRD (nm) |
|---|---|
| NA-Imp | 17.1 |
| NA | 22.0 |
| Cu-NA | 24.2 |
| Mn-NA-Imp | 14.9 |
| Mn-NA | 21.5 |

### 5.1.1.2 Nitrogen physisorption

The surface area of catalysts were characterized by BET (Brunauer-Emmett-Teller) method. BET surface areas, pore volume, and pore size of the $Ni/Al_2O_3$ catalysts which were prepared by solid-state reaction and the incipient wetness impregnation are summarized in Table 5.2. The surface areas of Ni-based catalysts with different promoters were ranged between 130-193 $m^2/g$. The modified nickel catalysts with Cu and Mn and the non-modified nickel catalysts can result in similar surface area. However, the catalysts prepared by the incipient wetness impregnation showed lower surface area. This suggests that some pores of alumina may be blocked by Ni-loaded particles. The Mn-NA-Imp presented the most decrease in BET surface area. Moreover, the pore volume of modified nickel catalysts with Cu and Mn were ranged between 0.15-0.21 $cm^3/g$. It was found that the Ni-based catalysts prepared by the solid-state reaction had higher pore volume and smaller pore size than the incipient wetness impregnation method. The Mn-NA-Imp indicated the most decrease of pore volume than the other nickel catalysts, illustrating that some pores of alumina were blocked by Ni-loaded particles [19].

Table 5.2  BET surface areas of unmodified and modified with manganese and copper promoters of nickel catalysts

| Sample | BET surface area ($m^2/g$) | Average pore volume ($cm^3/g$) | Average pore size (nm) |
|--------|------------------------------|----------------------------------|--------------------------|
| NA-Imp | 131 | 0.17 | 4.55 |
| NA | 193 | 0.20 | 4.22 |
| Cu-NA | 186 | 0.19 | 4.17 |
| Mn-NA-Imp | 130 | 0.15 | 5.09 |
| Mn-NA | 192 | 0.21 | 4.31 |

### 5.1.1.3 Hydrogen temperature program reduction ($H_2$-TPR)

Hydrogen temperature program reduction technique was carried out to determine the reduction behaviors of Ni-based catalysts samples prepared by the solid-state reaction between the mixture of nickel nitrate, gibbsite, and promoter, and the incipient wetness impregnation method. In general, the TPR profiles depend on the metal-support interaction, variance in metal particle size, and support porous structure which, resulted in different reducibility of nickel species on the support [14, 19]. The TPR profiles for the Ni-based catalysts samples are shown in Figure 5.2.

**Table 5.3** TPR data of unmodified and modified with manganese and copper promoters of nickel catalysts

| Sample | $T_m$ ($^\circ$C) | | | $H_2$ consumption (umol/g) |
|---|---|---|---|---|
| | $1^\circ$ peak | $2^\circ$ peak | $3^\circ$ peak | |
| NA-Imp | 239 | 391 | 574 | 21155.3 |
| NA | 251 | 425 | 640 | 19496.5 |
| Cu-NA | 225 | 285 | 603 | 21048.5 |
| Mn-NA-Imp | 287 | 351 | 537 | 23093.3 |
| Mn-NA | 253 | 362 | 412 | 22663.6 |

According to the TPR profiles, the reducibility of NiO particles could be classified into three types: 1-type is the bulk NiO, 2-type is weakly interaction between Ni with alumina, and 3-type is strongly interaction between Ni with alumina [11]. The TPR results of the nickel catalysts with manganese and copper promoters were compared the peak temperatures and the calculated $H_2$ consumption are summarized in Table 5.3.

Figure 5.2  The TPR profiles of Ni/Al$_2$O$_3$ catalysts with different promoters,
NA-Imp (a), NA (b), Cu-NA (c), Mn-NA-Imp (d), Mn-NA (e).

The three peak temperatures centered at 225-287$^\circ$C, 285-425$^\circ$C, and 412-640$^\circ$C, respectively. The first (1$^\circ$) peak temperatures of all Ni catalysts were like the TPR profile of bulk nickel oxide that, the NiO particles separated from the alumina support. The second (2$^\circ$) peak temperatures shifted down when the catalysts were promoted with manganese and copper. It is suggested that Mn and Cu promoting catalysts incurred a weaker interaction between NiO and alumina support. Moreover, the TPR profile of Cu promoter on the Ni/Al$_2$O$_3$ catalyst prepared by solid-state reaction, showed a high reduction temperature in the third (3$^\circ$) peak temperatures. Thus the NiO formatted could be reduced at higher reduction temperature. For H$_2$ consumption, it was found that the modified Ni catalysts prepared by either the

solid-state reaction or the incipient wetness impregnation showed higher $H_2$ consumption than non-modified Ni catalysts.

### 5.1.1.4 Scanning electron microscopy analyses (SEM)

The morphology of the $Ni/Al_2O_3$ catalysts with different promoters which were prepared by the solid-state reaction between nickel nitrate, gibbsite, and promoter, and the incipient wetness impregnation are displayed by SEM. The SEM images of the nickel catalysts with promoters (manganese, and copper) received from the solid-state reaction and the incipient wetness impregnation are shown in Figure 5.3. The non-modified and modified Ni catalysts had non-uniform particle size and shape. It is found that the additive manganese and copper can result in agglomeration of nickel species on surface.
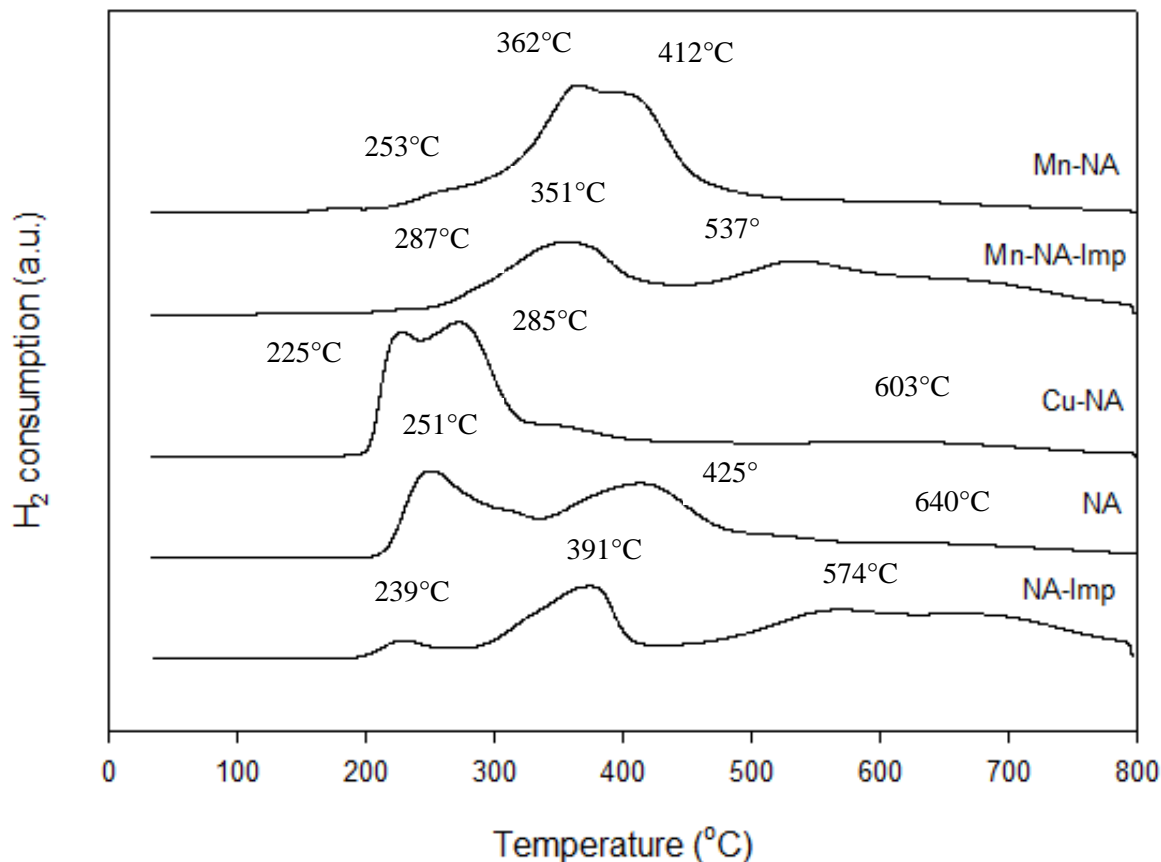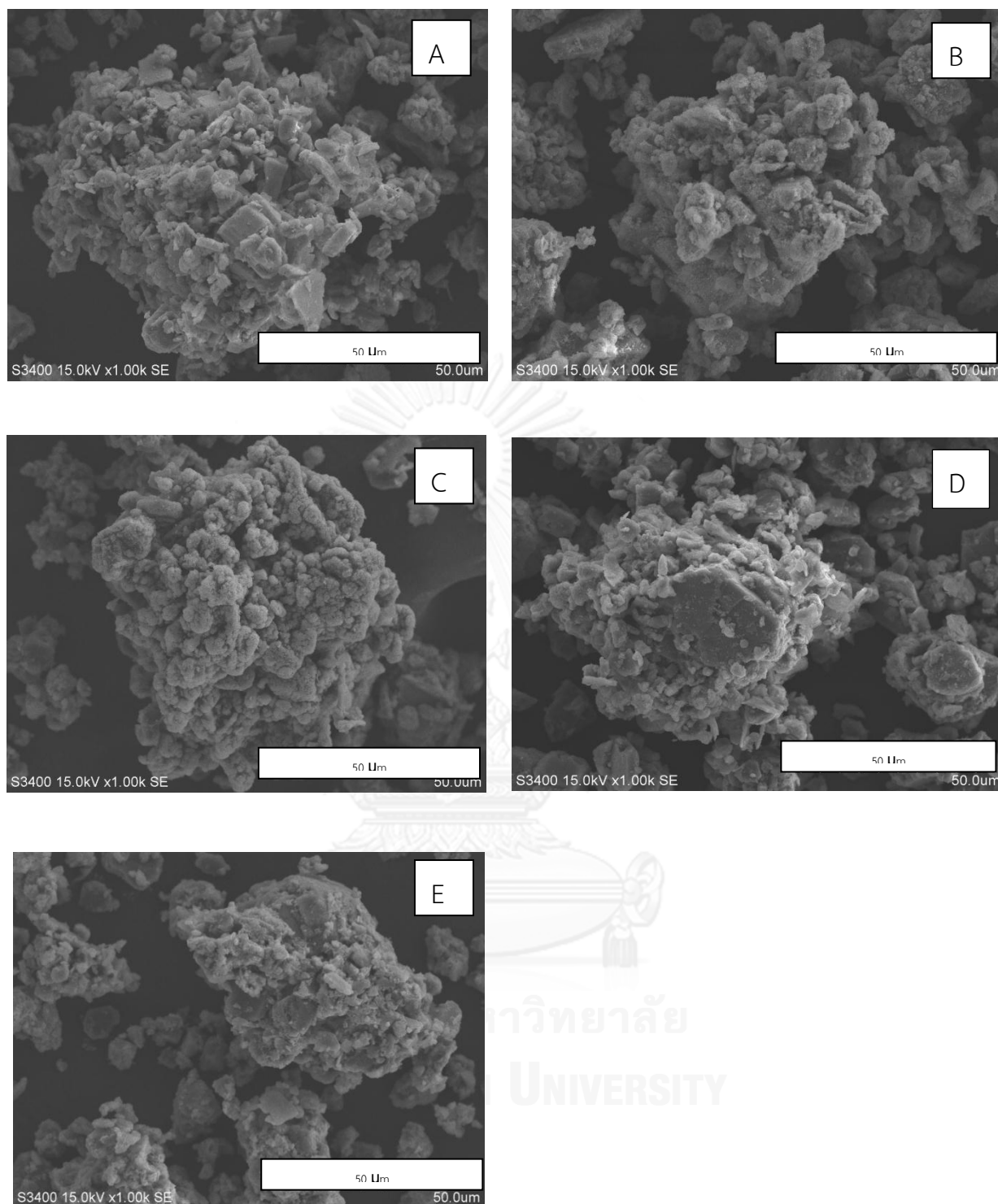
Figure 5.3  The SEM images of Ni/Al$_2$O$_3$ catalysts with different promoters,
NA-Imp (A), NA (B), Cu-NA (C), Mn-NA-Imp (D), Mn-NA (e).

### 5.1.1.5 Hydrogen chemisorption

The amount of active sites of nickel metals on the Ni/Al$_2$O$_3$ catalysts with manganese and copper promoters which were prepared by the solid-state reaction between nickel nitrate, gibbsite, and promoter, and the incipient wetness impregnation were analyzed by the H$_2$ chemisorption. Table 5. shows the H$_2$ chemisorption of the nickel active sites of the Ni/Al$_2$O$_3$ catalysts incurred from the solid-state reaction and the incipient wetness impregnation after calcination at 500°C and reduction at 400°C. The Ni active sites were ranged between 5.53-43.24 $\times 10^{18}$ molecules H$_2$/g cat in the order: Mn-NA-Imp > NA-Imp > Mn-NA > NA > Cu-NA. It was found that the H$_2$ chemisorption of Ni-based catalysts prepared by the incipient wetness impregnation were higher than the solid-state reaction. According to the average NiO crystallite size as measured from XRD, the NiO prepared from the incipient wetness impregnation were smaller than the solid-state reaction. Therefore, the NiO may be easier to reduce to nickel active sites. Besides, comparing the modified nickel catalysts with manganese and copper, the Ni catalyst promoted with manganese showed higher H$_2$ chemisorption and better dispersion on support than copper [20].

**Table 5.4  Hydrogen chemisorption results of unmodified and modified with manganese and copper promoters of nickel catalysts**

| Sample | H$_2$ chemisorption ($\times 10^{-18}$ molecules/g.cat) | % Dispersion |
|---|---|---|
| NA-Imp | 27.02 | 6.52 |
| NA | 9.12 | 2.21 |
| Cu-NA | 5.53 | 1.34 |
| Mn-NA-Imp | 43.24 | 10.50 |
| Mn-NA | 12.78 | 3.10 |

### 5.1.1.6 X-ray photoelectron spectroscopy (XPS)

The nickel species on the surface and the relative amount of element on the surface were analyzed by XPS technique. The catalysts were analyzed in the Ni 2p, Mn 2p, Cu 2p, Al 2p, O 1s, C 1s binding energy regions. The literature data of compound types of nickel are shown in Table 5.5. Following the binding energy, FWHM of Ni $2p_{3/2}$ and Al 2p, and the ratio of percentages of atomic concentration are shown in Table 5.6. The nickel in an oxidation state, the XPS spectra show that Ni $2p_{3/2}$ in NiO had lower binding energy than in $NiAl_2O_4$ at around 854 and 860 eV, respectively [21]. The binding energy of Ni $2p_{3/2}$ of the non-modified nickel catalysts prepared by the solid-state reaction (NA) were matched with NiO. For the non-modified nickel catalysts prepared by the incipient wetness impregnation (NA-Imp) were shifted towards higher binging energy. It can be indicated that the electron density on the nickel atoms of NA-Imp catalyst were lower than NA catalyst. It was probably the amorphous nickel oxide [22].

**Table 5.5  XPS data for the binding energy of nickel-containing reference materials [22].**

| Compound type | Ni $2p_{3/2}$ B.E. (eV) |
|---|---|
| Ni | 852.5-852.9 |
| NiO | 853.3-854.3 |
| $Ni_2O_3$ | 855.8–857.3 |
| $Ni(OH)_2$ | 855.6 |
| $NiCO_3$ | 854.7 |
| $Ni(CO)_4$ | 854.8–855.0 |

Comparing the modified nickel catalysts with manganese and copper, the one modified with Mn showed higher binging energy. That is the electron density on the

Ni atoms of the modified Ni catalysts with Mn was lower than the modified Ni catalysts with Cu [22]. For the atomic concentration of Ni/Al, comparing the Ni catalysts prepared by the solid-state reaction and prepared by the incipient wetness impregnation, it was found that the one prepared by the incipient wetness impregnation showed lower the amount of nickel on surface. The results are in accordance to the BET surface area and pore volume results.

Table 5.6  The binding energy, FWHM of Ni $2p_{3/2}$ and Al 2p, and the ratio of percentages of atomic concentration of the nickel catalysts.

| Sample | Ni (II) 2p3/2 | | Al 2p | | Atomic Conc % | | | |
|---|---|---|---|---|---|---|---|---|
| | B.E. (eV) | FWHM | B.E. (eV) | FWHM | Mn/Ni | Cu/Ni | Ni/Al | Al/O |
| NA-Imp | 856.1 | 4.151 | 75.8 | 2.041 | 0 | 0 | 0.294 | 0.55 |
| NA | 854.4 | 4.167 | 67.0 | 3.207 | 0 | 0 | 0.653 | 0.71 |
| Cu-NA | 854.9 | 4.207 | 67.1 | 3.382 | 0 | 0.047 | 0.669 | 0.62 |
| Mn-NA-Imp | 856.4 | 3.593 | 68.4 | 1.504 | 0.078 | 0 | 0.703 | 0.57 |
| Mn-NA | 857.0 | 3.868 | 69.3 | 3.037 | 0.105 | 0 | 0.760 | 0.35 |

**5.1.2 The catalytic activities of the Ni/Al$_2$O$_3$ catalysts in carbon dioxide hydrogenation**

The overall activities of the Ni/Al$_2$O$_3$ catalysts were studied in carbon dioxide hydrogenation reaction. Firstly, 0.1 g catalyst was packed in the quartz microreactor The total gas flow rate was 21.2 ml/min with the H$_2$/CO$_2$ ratio of 10/1. Secondly, the catalysts were reduced in flowing H$_2$ at 400°C for 4 h. Finally, the reaction was carried out at 500$^{\circ}$C and 1 atm total pressure.

The conversion and product selectivity during carbon dioxide hydrogenation reaction are shown in Table 5.7. The steady state of carbon dioxide hydrogenation of the Ni-based catalysts were ranging between 32.3-69.4% in the order: Mn-NA-Imp > Mn-NA > Cu-NA > NA-Imp > NA. It was found that the nickel promoted with

manganese catalysts prepared by either the solid-state reaction or the incipient wetness impregnation method showed the highest $CO_2$ conversion among the prepared $Ni/Al_2O_3$ catalysts. According to $H_2$ chemisorption, the amount of nickel active sites of Mn-NA-Imp catalysts were the highest the Ni active sites although the BET surface area of Mn-NA-Imp were the most decrease surface area and pore volume. Therefore the nickel particles may be located in the pore of alumina. According to XPS analyses, the nickel on surface of the Mn-NA-Imp catalysts were lower than the Mn-NA catalysts. Comparing the non-modified nickel catalysts, the one prepared by solid-state reaction exhibited slightly lower $CO_2$ conversion than the non-modified nickel prepared by the incipient wetness impregnation method. According to $H_2$ chemisorption, the amounts of nickel active sites of NA catalysts were lower than NA-Imp catalysts. However, promotion with manganese can result in similar $CO_2$ conversion during the 5 h time-on-stream, regardless of the preparation method used. The improved with manganese catalysts performances can be attributed to better dispersion of the NiO particles, according to the smaller NiO crystallite size found in the XRD patterns. That is the smaller NiO may be easier to reduce to active nickel particles. Moreover, comparing the catalysts promoted with manganese and copper, the one promoted with Mn exhibited a shift of the reduction temperature towards lower temperature than promoted with Cu, therefore, the reduction of NiO was easier. According to the NiO crystallite size, the modified Ni with Mn showed the smaller NiO crystallite size. For the catalysts prepared by the solid-state reaction, reducibility of the catalysts were also increased with the addition of either Cu or Mn promoters. According to the higher $H_2$ consumptions found in the $H_2$-TPR technique.

Table 5.7  The conversion, and product selectivity during $CO_2$ hydrogenation at initial and steady-state conditions of nickel catalysts after calcination at 500 $^{\circ}$C

| Sample | Conversion [a] (%) | | Product selectivity [a] (%) | | | |
|---|---|---|---|---|---|---|
| | Initial [b] | Steady state [c] | Initial [b] | | Steady state [c] | |
| | | | CH$_4$ | CO | CH$_4$ | CO |
| NA-Imp | 44.7 | 37.5 | 5.5 | 94.5 | 4.8 | 95.2 |
| NA | 34.5 | 32.3 | 8.3 | 91.7 | 4.8 | 95.2 |
| Cu-NA | 48.8 | 58.8 | 100 | 0 | 100 | 0 |
| Mn-NA-Imp | 68.2 | 69.4 | 100 | 0 | 100 | 0 |
| Mn-NA | 67.3 | 67.2 | 100 | 0 | 100 | 0 |

[a] $CO_2$ hydrogenation was carried out at 500 $^{\circ}$C, 1 atm, $H_2/CO_2$ = 10.

[b] After 30 min of reaction.

[c] After 4 h of reaction.
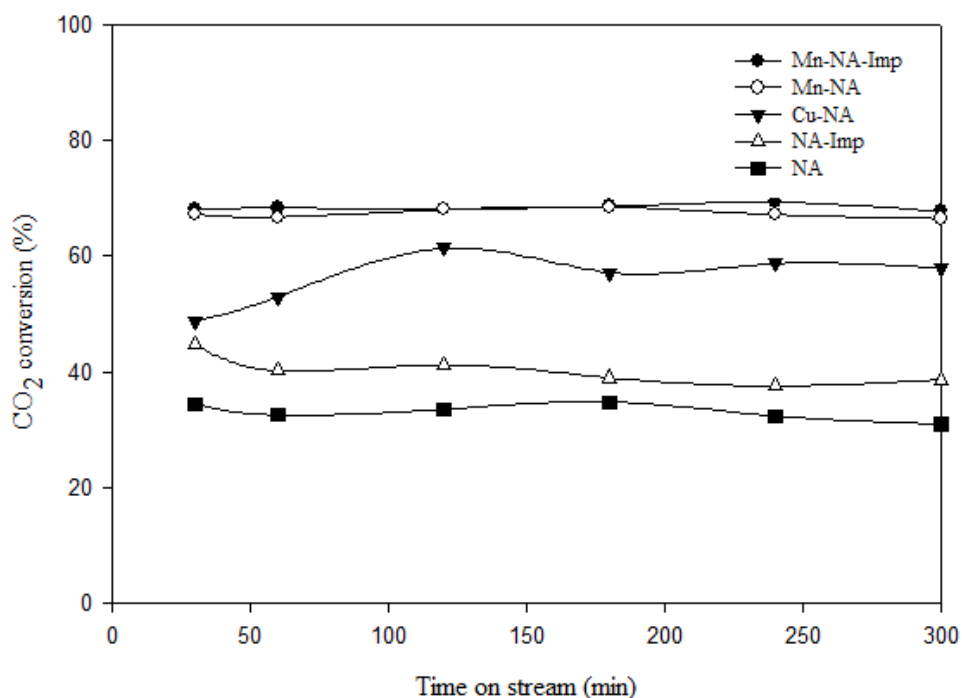


Figure 5.4  Carbon dioxide conversion of Ni/Al$_2$O$_3$ catalysts with different promoters

## 5.2  Effect of the amounts of Mn promoters

### 5.2.1 Catalysts characterization

The label used for the catalysts are as shown:

**X-Mn-NA** is referred to the catalyst prepared by solid-state reaction which was composed of a mixture of nickel nitrate, gibbsite, and the percent loading of manganese acetate.

### 5.2.1.1 X-ray diffraction (XRD)

The XRD patterns of 20 wt% $Ni/Al_2O_3$ catalysts with various percents loading of manganese (0, 0.25, 0.5, 1, 2wt% Mn) calcined at 500°C in air which were prepared by the solid-state reaction using the mixture of nickel nitrate, gibbsite, and manganese acetate are shown in Figure 5.5. The scans were recorded in the $2\theta$ range of 10-90$^{\circ}$. The XRD diffraction peaks of all the Ni-based catalysts presented at $2\theta$ degrees 37.2$^{\circ}$, 43.2$^{\circ}$, 62.8$^{\circ}$, 75.3$^{\circ}$, 79.5$^{\circ}$, that referred to the metal NiO crystalline phase [4]. Their patterns were not shown the other Ni species. There were no difference among the catalysts that various percent loading of manganese. However, the XRD patterns were not detected the manganese oxides crystalline phase, which may be highly dispersed on the support. Moreover, the highest percent loading of manganese on the Ni-based catalysts resulted in a of decrease the NiO crystallite size. The 2 wt% loading of manganese presented in the lowest intensity of XRD patterns.
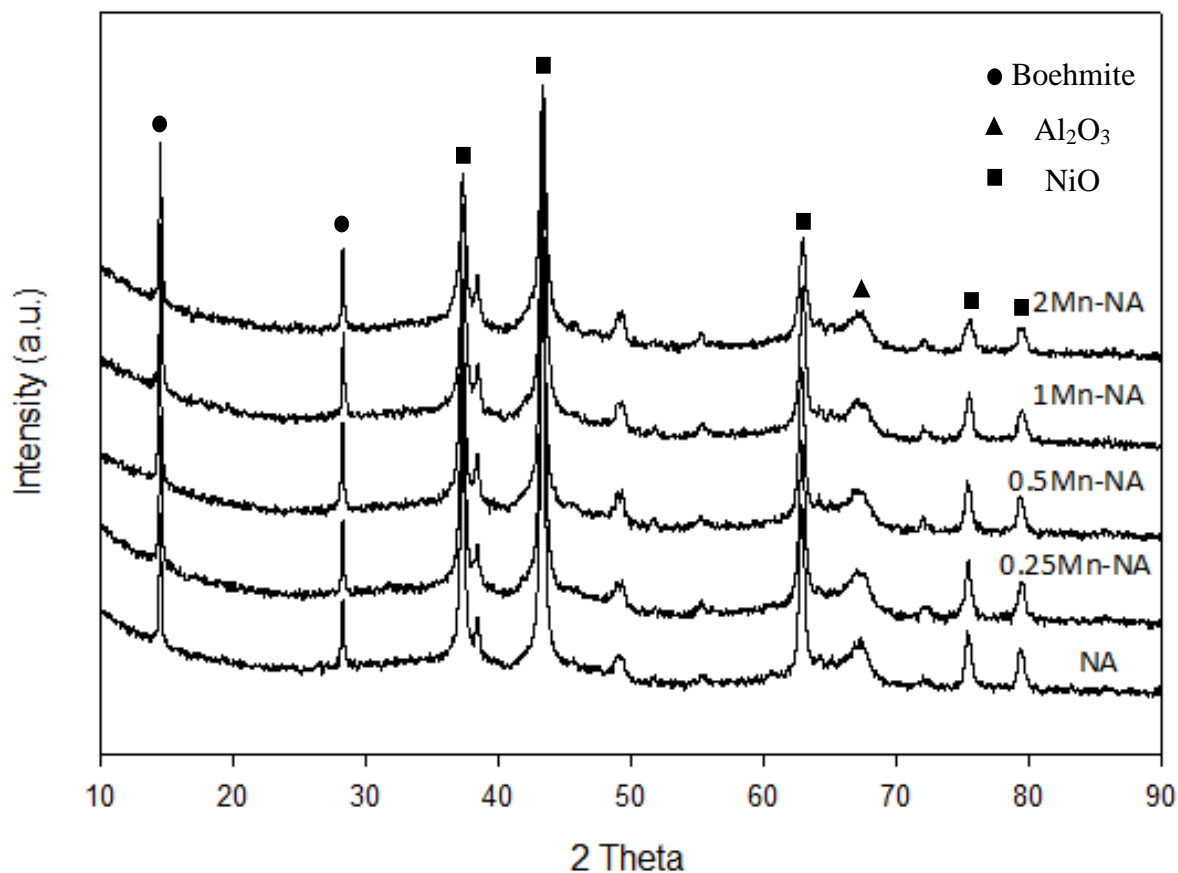
Figure 5.5  The XRD patterns of 20 wt% Ni/Al$_2$O$_3$ catalysts with various percent loading of manganese, ● = Boehmite; ■ = NiO; ▲ = Al$_2$O$_3$, NA (a), 0.25 Mn-NA (b), 0.5 Mn-NA (c), 1 Mn-NA (d), 2 Mn-NA(e).

### 5.2.1.2 Nitrogen physisorption

BET surface areas, pore volume, and pore size of the 20 wt% nickel based catalysts with various percents loading of manganese (0, 0.25, 0.5, 1, 2wt% Mn) which prepared by solid-state reaction are summarized in Table 5.8. The surface areas of Ni catalysts with percent loading of Mn were ranged between 163-193 m$^2$/g. The modified nickel catalysts with manganese presented depressed the surface area. Because some pores of alumina support may be blocked after solid state reaction. However, it is found that the addition of loading Mn showed the higher surface area.

The 0.5 Mn-NA indicated the highest BET surface area at 193 $m^2$/g. Because the Mn promoters may be diffuse of Ni and Mn on support [11]. Increase in 2 wt% Mn loading showed the lower surface area. The pore volume of various loaded nickel catalysts with Mn were ranged between 0.19-0.21 $cm^3$/g. It is found that the increase of loading manganese had a little impact on the pore volume.

Table 5.8 BET surface areas of the 20 wt% nickel based catalysts with various percent loading of manganese (0, 0.25, 0.5, 1, 2wt% Mn).

| Sample | BET surface area ($m^2$/g) | Average pore volume ($cm^3$/g) | Average pore size (nm) |
|---|---|---|---|
| NA | 193 | 0.20 | 4.22 |
| 0.25 Mn-NA | 163 | 0.21 | 5.03 |
| 0.5 Mn-NA | 193 | 0.19 | 4.02 |
| 1 Mn-NA | 192 | 0.21 | 4.31 |
| 2 Mn-NA | 167 | 0.19 | 4.66 |

### 5.2.1.3 Hydrogen temperature program reduction ($H_2$-TPR)

Hydrogen temperature program reduction technique was used to determine the reduction behaviors of the 20 wt% nickel-based catalysts samples with various percent loading of manganese (0, 0.25, 0.5, 1, 2 wt% Mn) which prepared by solid-state reaction. The TPR profiles for the 20 wt% $Ni/Al_2O_3$ catalysts samples with Mn promoters are summarized in Figure 5.6.

Table 5.9   TPR data of the Ni/Al$_2$O$_3$ catalysts with various percent loading of manganese promoters

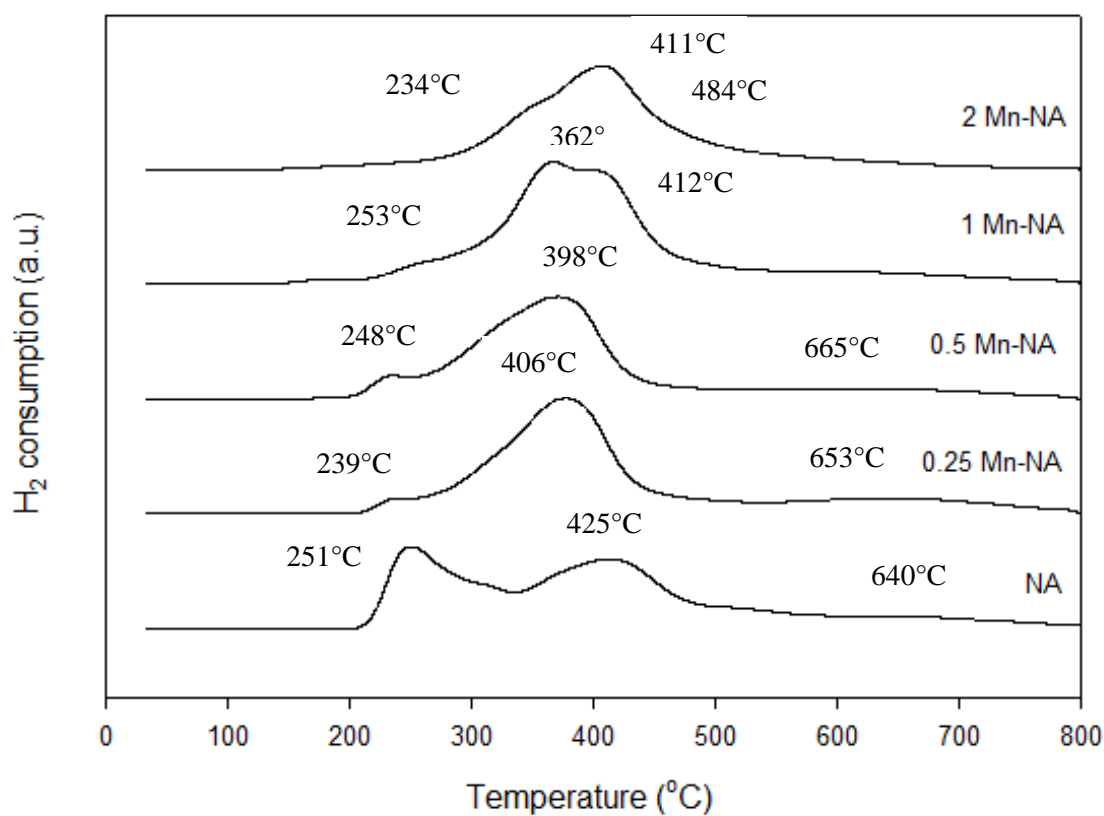| Sample | T$_m$ ($^o$C) | | | H$_2$ consumption (umol/g) |
|---|---|---|---|---|
| | 1$^o$ peak | 2$^o$ peak | 3$^o$ peak | |
| NA | 251 | 425 | 640 | 19496.5 |
| 0.25 Mn-NA | 239 | 406 | 653 | 20638.3 |
| 0.5 Mn-NA | 248 | 398 | 665 | 19745.7 |
| 1 Mn-NA | 253 | 362 | 412 | 22663.6 |
| 2 Mn-NA | 234 | 411 | 484 | 19195.7 |



Figure 5.6   The TPR profiles of 20 wt% Ni/Al$_2$O$_3$ catalysts with various percent loading of manganese, NA (a), 0.25 Mn-NA (b), 0.5 Mn-NA (c), 1 Mn-NA (d), 2 Mn-NA (e).

The TPR results of the nickel-based catalysts with various percent loading of manganese promoters were compared. The peak temperatures and the calculated $H_2$ consumption are presented in Table 5.9. The three peak temperatures centered at 234-253$^\circ$C, 362-425$^\circ$C, and 412-665$^\circ$C, respectively. The first (1$^\circ$) peak temperatures of modified nickel catalysts showed the nearby reduction temperature. These peak temperatures presented the reduction of bulk NiO. The second (2$^\circ$) peak temperatures showed a shift down of the reduction temperature when increased amount of manganese loading. The 1 Mn-NA catalyst exhibited the lowest reduction temperature either the second (2$^\circ$) or the third (3$^\circ$) peak temperatures (362$^\circ$C, and 412$^\circ$C, respectively). The manganese promoting catalysts showed a weaker interaction between metal and support. However, increase in the Mn loadings (2 wt% Mn) showed higher reduction temperature in the second (2$^\circ$) peak. That is the nickel oxides were reduced at higher reduction temperature. For $H_2$ consumption, it was found that the promoted nickel catalysts with manganese prepared by the solid-state reaction exhibited higher $H_2$ consumption. Therefore, the nickel catalysts can be higher reduced. However, the 2 wt% Mn loadings showed lower $H_2$ consumption. That is the nickel oxides were lower reduced when manganese loading increase.

**5.2.1.4 Scanning electron microscopy analyses (SEM)**

The morphology of the 20 wt% nickel loaded catalysts with various percent loading of manganese (0, 0.25, 0.5, 1, 2wt% Mn) which prepared by solid-state reaction were analyzed by SEM technique in Figure 5.7. All the Ni-based catalysts had uneven shape and size. The promotion with manganese on nickel catalysts resulted in more agglomeration of nickel particles on surface. Moreover, the modified Ni catalysts with different loading, of Mn showed no difference in particle size and shape.
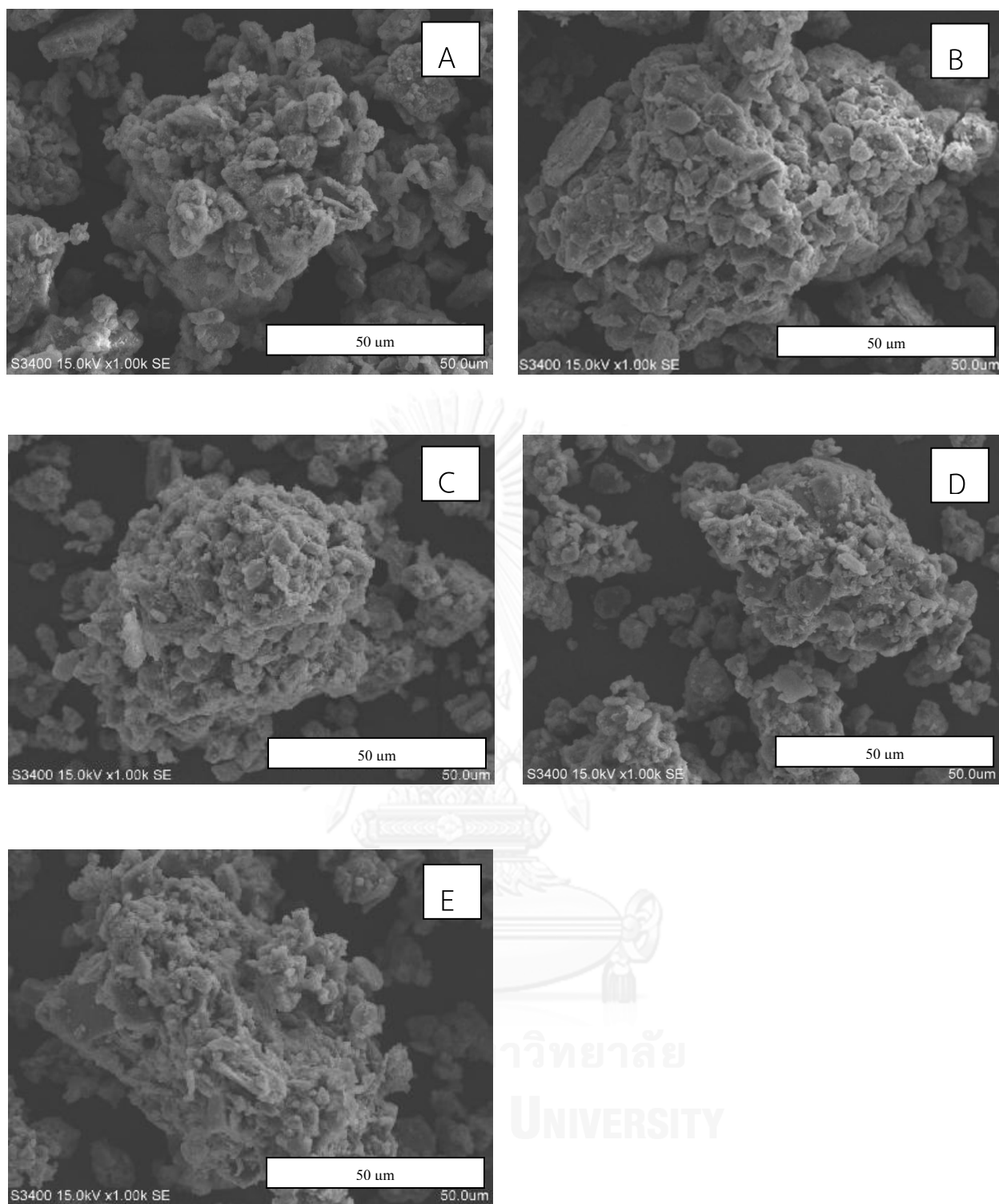
Figure 5.7  The SEM images of the 20 wt% nickel loaded catalysts with various
percent loading of manganese, NA (A), 0.25 Mn-NA (B), 0.5 Mn-NA (C),
1 Mn-NA (D), 2 Mn-NA (e).

### 5.2.1.5 Hydrogen chemisorption

The Ni active sites of the 20 wt% Ni-based catalysts with various percent loading of manganese (0, 0.25, 0.5, 1, 2wt% Mn) which prepared by solid-state reaction between nickel nitrate, gibbsite, and manganese acetate after calcination at 500°C and reduction at 400°C are summarizes in Table 5.10. The nickel active sites were ranged between 9.12-13.76 ×$10^{18}$ molecules $H_2$/g cat in the order: 2 Mn-NA > 0.5 Mn-NA > 1 Mn-NA > 0.25 Mn-NA > NA. It was found that the $H_2$ chemisorption of the modified Ni catalysts with manganese prepared by the solid-state reaction were higher than the non-modified Ni catalysts. Moreover, the manganese promoters also increased dispersion of the Ni active sites. However, increasing the amount of manganese promoters from 0.25 to 2 wt% can result in similar $H_2$ chemisorption.

**Table 5.10** Hydrogen chemisorption results of the Ni/Al$_2$O$_3$ catalysts with various percent loading of manganese promoters

| Sample | $H_2$ chemisorption (×$10^{-18}$ molecules/g.cat) | % Dispersion |
| --- | --- | --- |
| NA | 9.12 | 2.21 |
| 0.25 Mn-NA | 12.47 | 3.03 |
| 0.5 Mn-NA | 13.68 | 3.32 |
| 1 Mn-NA | 12.78 | 3.10 |
| 2 Mn-NA | 13.76 | 3.34 |

### 5.2.1.6 X-ray photoelectron spectroscopy (XPS)

The nickel species on the surface and the relative amount of element on the surface were analyzed by XPS technique. The catalysts were analyzed in the Ni 2p, Mn 2p, Al 2p, O 1s, C 1s binding energy regions. The binding energy, FWHM of Ni 2p$_{3/2}$ and Al 2p, and the ratio of percentages of atomic concentration are exhibited in

Table 5.11. The nickel was in an oxidation state. The XPS spectra show that Ni $2p_{3/2}$ in NiO had lower binding energy than in $NiAl_2O_4$. It was found that the binding energy of Ni $2p_{3/2}$ of the non-modified nickel catalysts prepared by the solid-state reaction (NA) were matched with NiO. For the modified nickel catalysts by manganese prepared by the solid-state reaction were shifted towards higher binding energies. For the atomic concentration of Ni/Al, comparing the non-modified Ni catalysts and modified Ni catalysts with manganese prepared by the solid-state reaction, it was found that the modified Ni catalysts showed higher the amount of nickel on surface. However, increasing the amounts of manganese loading can result in similar atomic concentration of Ni/Al on surface.

**Table 5.11  The binding energy, FWHM of Ni $2p_{3/2}$ and Al 2p, and the ratio of percentages of atomic concentration of the non-modified and modified nickel catalysts.**

| Sample | Ni (II) $2p_{3/2}$ | | Al 2p | | Atomic Conc % | | |
|---|---|---|---|---|---|---|---|
| | B.E. (eV) | FWHM | B.E. (eV) | FWHM | Mn/Ni | Ni/Al | Al/O |
| NA | 854.4 | 4.167 | 67.0 | 3.207 | 0 | 0.653 | 0.71 |
| 0.25 Mn-NA | 857.4 | 3.961 | 69.7 | 2.595 | 0.015 | 0.823 | 0.55 |
| 0.5 Mn-NA | 856.0 | 3.927 | 68.2 | 2.766 | 0.044 | 0.716 | 0.62 |
| 1 Mn-NA | 857.0 | 3.868 | 69.3 | 3.037 | 0.105 | 0.759 | 0.35 |
| 2 Mn-NA | 856.0 | 3.971 | 68.6 | 3.253 | 0.104 | 0.638 | 0.73 |

**5.2.2 The catalytic activities of the $Ni/Al_2O_3$ catalysts with various percent loading of manganese in carbon dioxide hydrogenation**

The overall activities of the 20 wt% $Ni/Al_2O_3$ catalysts with various percent loading of manganese (0, 0.25, 0.5, 1, 2wt% Mn) which prepared by solid-state reaction were studied in $CO_2$ hydrogenation reaction. Firstly, using 0.1 g catalyst packed in the quartz microreactor The total gas flow rate was 21.2 ml/min with the

$H_2/CO_2$ ratio of 10/1. Secondly, the catalysts were reduced in flowing $H_2$ at 400°C for 4 h. Finally, the reaction was carried out at 500°C and 1 atm total pressure.

The conversion and product selectivity during carbon dioxide hydrogenation reaction are presented in Table 5.12. The steady state of $CO_2$ hydrogenation of the 20 wt% Ni catalysts were ranging between 32.3-67.2% in the order: 2 Mn-NA = 1 Mn-NA > 0.5 Mn-NA > 0.25 Mn-NA > NA. It was found that the non-modified nickel catalysts showed the lowest $CO_2$ conversion than the modified nickel prepared by solid-state reaction. According to $H_2$ chemisorption, the amount of nickel active sites of NA catalysts were the lowest the Ni active sites and dispersion of the Ni active sites. Moreover, the larger NiO crystallite size found in the XRD patterns which the one may be difficult to reduce to active nickel particles. The non-modified Ni catalysts showed a shift of the reduction temperature towards higher temperature than modified Ni catalysts , therefore, the reduction of NiO was more difficult. Comparing the modified nickel catalysts, increasing the amount of manganese loading showed higher $CO_2$ conversion. According to $H_2$ chemisorption, the amount of nickel active sites exhibited slightly higher Ni active sites. However, it was found that the amount of manganese loading between 0.5-2 wt% Mn which can result in similar $CO_2$ conversion during the 5 h time-on-stream consistent with the result in similar the amount of nickel active sites and dispersion of nickel species on support. Further reducibility of the modified nickel catalysts can result in similar the reduction temperature. Therefore regardless of the amount of manganese promoters used (0.5-2 wt% Mn, all the modified catalysts showed similar $CO_2$ conversion.

Table 5.12 The conversion, and product selectivity during $CO_2$ hydrogenation at initial and steady-state conditions of nickel catalysts with various percent loading of manganese after calcination at 500 $^{\circ}$C

| Sample | Conversion [a] (%) | | Product selectivity [a] (%) | | | |
|---|---|---|---|---|---|---|
| | Initial [b] | Steady state [c] | Initial [b] | | Steady state [c] | |
| | | | $CH_4$ | CO | $CH_4$ | CO |
| NA | 34.5 | 32.3 | 8.3 | 91.7 | 4.8 | 95.2 |
| 0.25 Mn-NA | 58.2 | 46.9 | 100 | 0 | 100 | 0 |
| 0.5 Mn-NA | 65.3 | 66.1 | 100 | 0 | 100 | 0 |
| 1 Mn-NA | 67.3 | 67.2 | 100 | 0 | 100 | 0 |
| 2 Mn-NA | 69.5 | 67.2 | 100 | 0 | 100 | 0 |

[a] $CO_2$ hydrogenation was carried out at 500 $^{\circ}$C, 1 atm, $H_2/CO_2$ = 10.

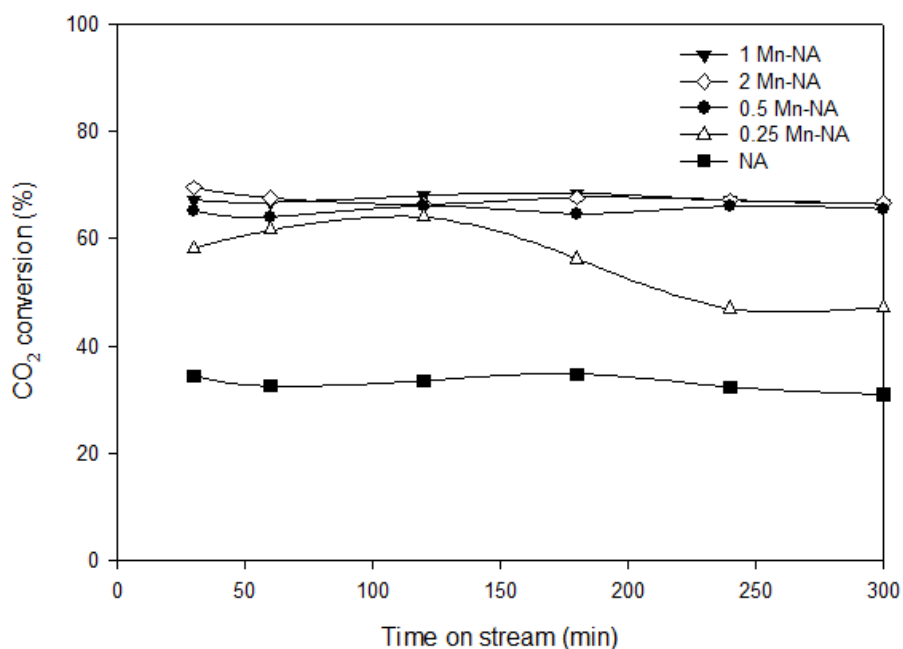[b] After 30 min of reaction.

[c] After 4 h of reaction.



Figure 5.8 Carbon dioxide conversion of $Ni/Al_2O_3$ catalysts with manganese promoters

## 5.3  Effect of the amounts of nickel

### 5.3.1 Catalysts characterization

The label used for the catalysts are as shown:

**X-NA-Mn** is referred to the catalysts prepared by solid-state reaction which composed of a mixture of manganese acetate, gibbsite, and the percent loading of nickel nitrate.

#### 5.3.1.1 X-ray diffraction (XRD)

The XRD patterns of the 0.5wt% Mn modified on Ni catalysts with various percent loading of nickel (5, 10, 15, 20 wt% Ni) calcined at 500℃ in air using the mixture of nickel nitrate, gibbsite, and manganese acetate which prepared by the solid-state reaction are shown in Figure 5.9. The XRD diffraction peaks of all the Ni-loaded catalysts exhibited at $2\theta$ degrees $37.2^{\circ}$, $43.2^{\circ}$, $62.8^{\circ}$, $75.2^{\circ}$, $79.3^{\circ}$, which were attributed to the metal NiO phase. All the catalysts showed the pattern of the NiO. However, the lower amount of percent loading of nickel on the Ni-based catalysts resulted in a decrease in the intensity of XRD patterns. The 5 wt% loading of nickel showed the lowest NiO XRD peak intensity.
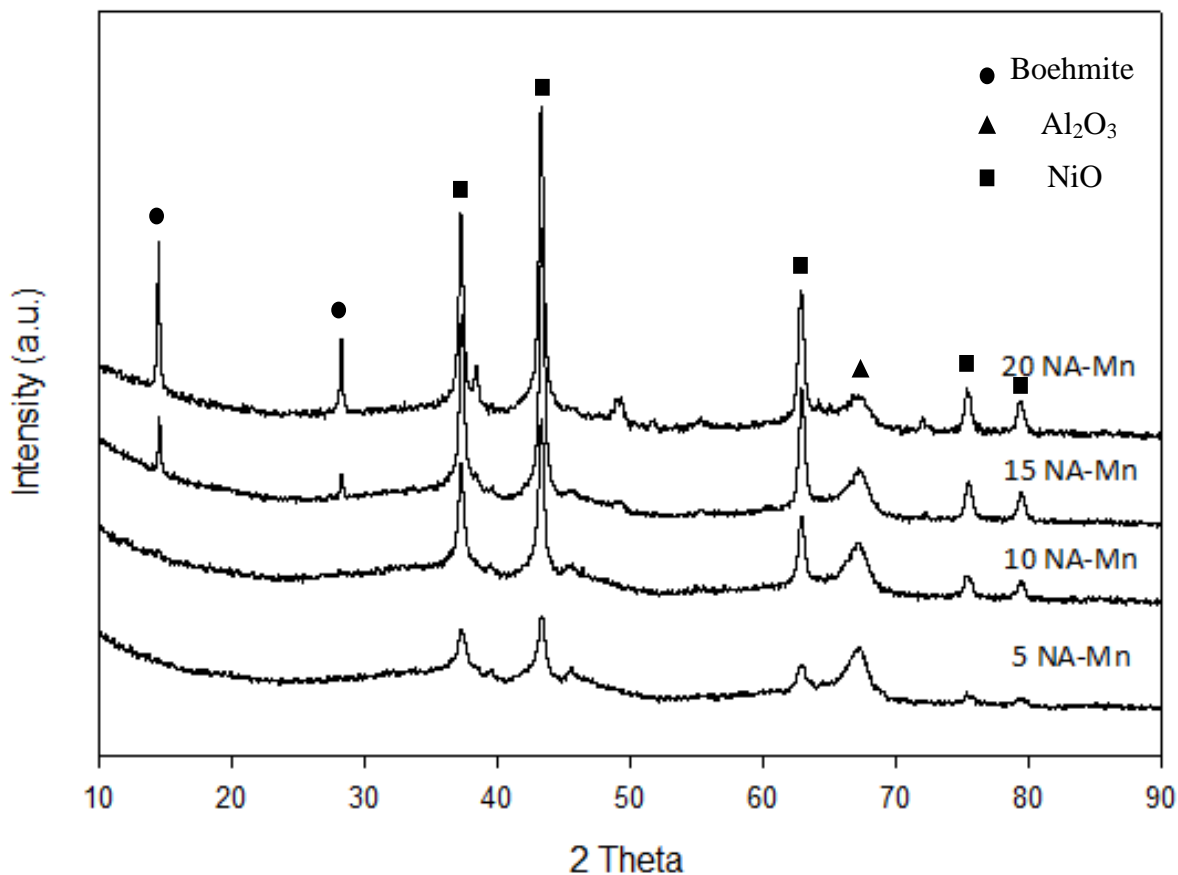
**Figure 5.9** The XRD patterns of the 0.5wt% Mn modified Ni catalysts with
various percent loading of nickel, ● = Boehmite; ■ = NiO; ▲ = $Al_2O_3$,
5 NA-Mn (a), 10 NA-Mn (b), 15 NA-Mn (c), 20 NA-Mn (d).

### 5.3.1.2 Nitrogen physisorption

BET surface areas, pore volume, and pore size of the 0.5wt% Mn modified on Ni catalysts with various percent loading of nickel (5, 10, 15, 20 wt% Ni) which prepared by solid-state reaction are summarized in Table 5.13. The surface areas of all $Ni/Al_2O_3$ catalysts with Mn promoters were ranged between 178-201 $m^2$/g. It was found that the increase of amount of nickel on alumina promoted by 0.5 wt% manganese showed cumulative the surface area. Because the further active nickel may be spread on the space for the pores of $Al_2O_3$ support. However, 5 wt% Ni modified catalysts showed the highest BET surface area at 201 $m^2$/g. Suggesting that

the few nickel may be not spread on gibbsite support during solid state reaction therefore, the BET surface area possibly showed the surface area of support. Moreover, the pore volume of various loaded nickel catalysts were ranged between 0.19-0.22 cm$^3$/g. The increase of loading nickel had a few variation of pore volume.

Table 5.13  BET surface areas of the 0.5 wt% Mn modified on Ni catalysts with various percent loading of nickel (5, 10, 15, 20 wt% Ni)

| Sample | BET surface area (m$^2$/g) | Average pore volume (cm$^3$/g) | Average pore size (nm) |
|---|---|---|---|
| 5 NA-Mn | 201 | 0.21 | 4.28 |
| 10 NA-Mn | 178 | 0.22 | 4.91 |
| 15 NA-Mn | 179 | 0.22 | 5.00 |
| 20 NA-Mn | 193 | 0.19 | 4.02 |

### 5.3.1.3 Hydrogen temperature program reduction (H$_2$-TPR)

Hydrogen temperature program reduction technique was employed to determine the reduction behaviors of the 0.5 wt% Mn modified on nickel catalysts with various percent loading of Ni (5, 10, 15, 20 wt% Ni) which prepared by solid-state reaction. The TPR profiles for the 0.5 wt% Mn modified on Ni/Al$_2$O$_3$ catalysts are summarized in Figure 5.10.

The TPR results of the 0.5 wt% Mn promoted on nickel catalysts with various percent loading of nickel were compared in terms of the peak temperatures and the calculated H$_2$ consumption as shown in Table 5.14. The three peak temperatures centered at 235-377$^{\circ}$C, 398-611$^{\circ}$C, and 665-746$^{\circ}$C, respectively. The (1$^{\circ}$) peak temperatures of all the nickel catalysts presented the reduction temperature of bulk nickel oxide [11]. The second (2$^{\circ}$) peak temperatures were shifted toward lower reduction temperature when the amount of nickel metal loading increased.

Table 5.14  TPR data of the manganese modified on Ni catalysts with various percent loading of nickel

| Sample | $T_m$ ($^o$C) | | | $H_2$ consumption |
|---|---|---|---|---|
| | $1^o$ peak | $2^o$ peak | $3^o$ peak | (umol/g) |
| 5 NA-Mn | 377 | 611 | 715 | 8628.8 |
| 10 NA-Mn | 376 | 596 | 746 | 14332.6 |
| 15 NA-Mn | 235 | 399 | 672 | 16994.1 |
| 20 NA-Mn | 248 | 398 | 665 | 19745.7 |

The 20 NA-Mn catalyst showed the lowest reduction temperature either the second ($2^o$) or the third ($3^o$) peak temperatures ($398^o$C, and $665^o$C, respectively). Thus, the reduction of nickel oxide was easier. For $H_2$ consumption, it was found that the increase of nickel metals on Ni-based catalysts prepared by the solid-state reaction indicated higher $H_2$ consumption. That is the nickel-based catalysts can be higher reduced. The 20 NA-Mn catalysts displayed the highest $H_2$ consumption.

**Figure 5.10** The TPR profiles of 0.5 wt% Mn modified on nickel catalysts with various percent loading of Ni, 5 NA-Mn (a), 10 NA-Mn (b), 15 NA-Mn (c), 20 NA-Mn (d).

### 5.3.1.4 Scanning electron microscopy analyses (SEM)

The morphology of the 0.5 wt% Mn modified on Ni catalysts with various percent loading of nickel (5, 10, 15, 20 wt% Ni) which prepared by solid-state reaction were investigated by SEM technique in Figure 5.11. All modified $Ni/Al_2O_3$ catalysts had irregular size and shape. Moreover, the increase of amount of nickel loading showed no difference in particle shape.
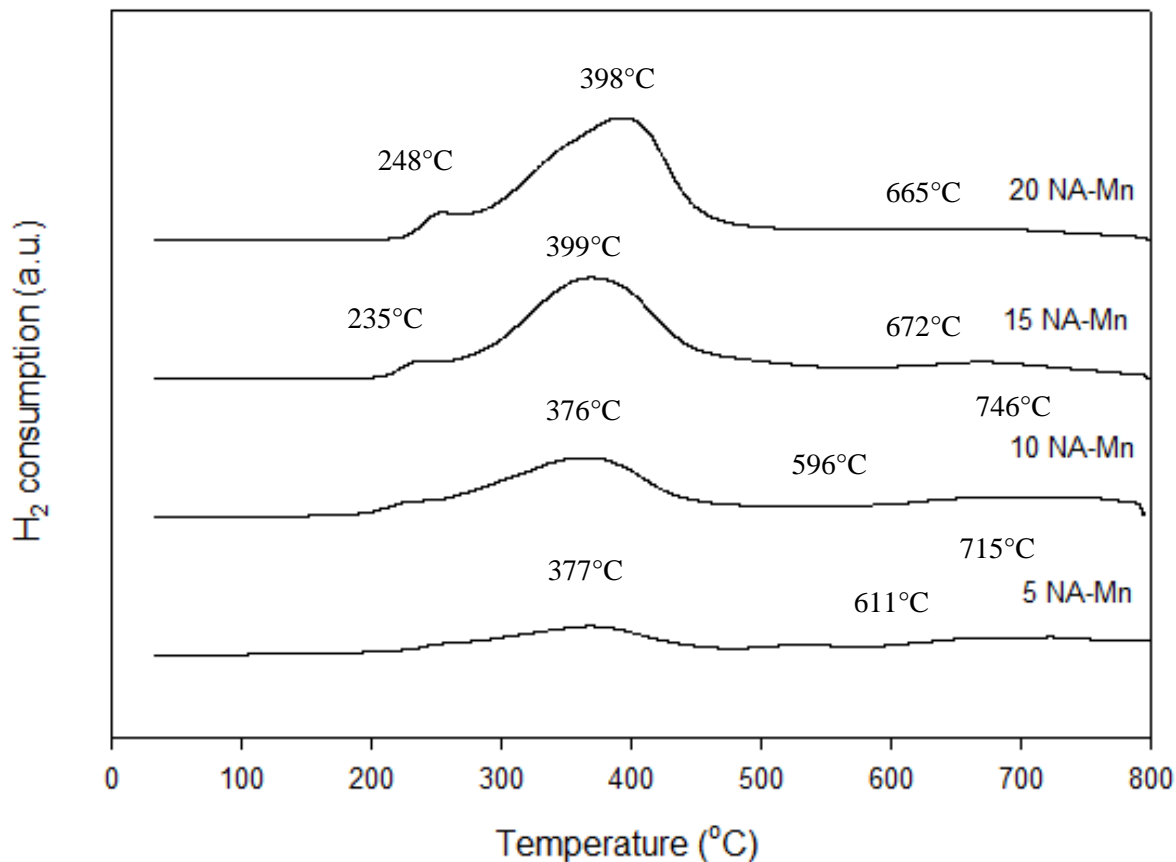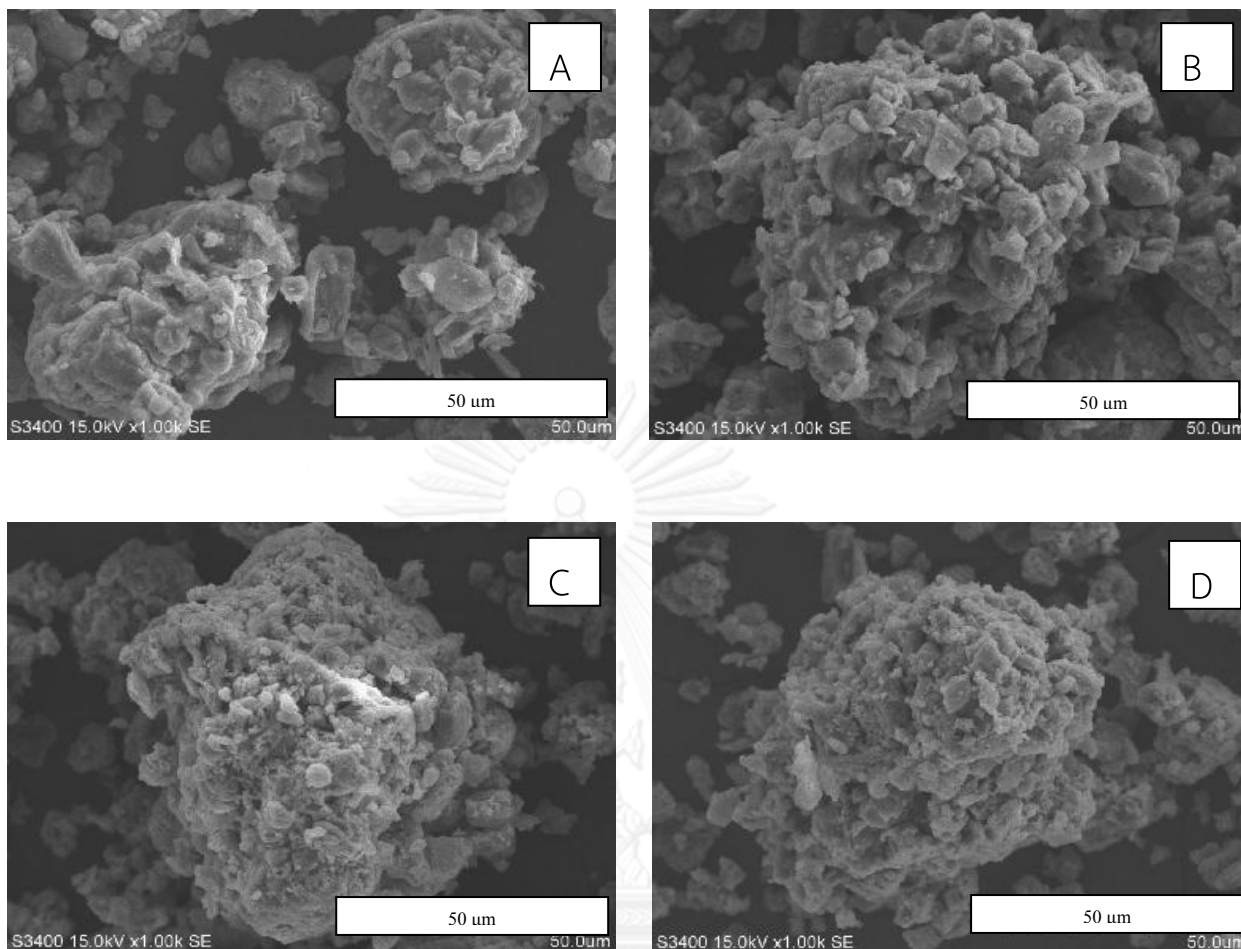
**Figure 5.11** The SEM images of the 0.5wt% Mn modified on Ni catalysts with various percent loading of nickel, 5 NA-Mn (A), 10 NA-Mn (B), 15 NA-Mn (C), 20 NA-Mn (D).

### 5.3.1.5 Hydrogen chemisorption

The active sites of nickel of the 0.5 wt% Mn modified on Ni-based catalysts with various percent loading of nickel (5, 10, 15, 20 wt% Ni) which prepared by solid-state reaction between manganese acetate, nickel nitrate, and gibbsite after calcination at 500°C and reduction at 400°C are summarizes in Table 5.15. The Ni active sites were ranged between 7.10-13.68 $\times 10^{18}$ molecules $H_2$/g cat in the order:

20 NA-Mn > 15 NA-Mn > 10 NA-Mn > 5 NA-Mn. It was found that the $H_2$ chemisorption of 20 wt% Ni modified catalysts showed the highest $H_2$ chemisorption at 13.68 $\times 10^{18}$ molecules $H_2$/g cat. That is, increasing the amount of the nickel catalysts with manganese promoters showed higher $H_2$ chemisorption. However, the higher nickels loading decreased the dispersion of the nickel active sites on support.

Table 5.15  Hydrogen chemisorption results of the manganese modified on Ni catalysts with various percent loading of nickel

| Sample | $H_2$ chemisorption ($\times 10^{-18}$ molecules/g.cat) | % Dispersion |
|---|---|---|
| 5 NA-Mn | 7.1 | 6.87 |
| 10 NA-Mn | 8.31 | 2.69 |
| 15 NA-Mn | 10.49 | 5.11 |
| 20 NA-Mn | 13.68 | 3.32 |

### 5.3.1.6 X-ray photoelectron spectroscopy (XPS)

The nickel species on the surface and the relative amount of element on the surface were analyzed by XPS technique. The catalysts were analyzed in the Ni 2p, Mn 2p, Al 2p, O 1s, C 1s binding energy regions. The binding energy, FWHM of Ni $2p_{3/2}$ and Al 2p, and the ratio of percentages of atomic concentration are shown in Table 5.16. It was found that the binding energy of Ni $2p_{3/2}$ of the 20 NA-Mn catalysts prepared by the solid-state reaction showed the lowest binding energies among all catalysts. However, decreasing the amounts of nickel loading in modified Ni catalysts were shifted towards higher binding energies. It can be indicated that the electron density on the nickel atoms of the 5, 10, 15 NA-Mn catalysts were lower than 20 NA-Mn catalyst. For the atomic concentration of Ni/Al, comparing the amounts of nickel loading prepared by the solid-state reaction, it was found that the 20 NA-Mn catalysts showed the highest the amounts of nickel on surface. Moreover, decreasing

the amounts of nickel loading can result in the decrease in the atomic concentration of Ni/Al on surface.

Table 5.16  The binding energy, FWHM of Ni $2p_{3/2}$ and Al 2p, and the ratio of percentages of atomic concentration of the non-modified and modified nickel catalysts.

| Sample | Ni (II) $2p_{3/2}$ | | Al 2p | | Atomic Conc % | | |
|---|---|---|---|---|---|---|---|
| | B.E. (eV) | FWHM | B.E. (eV) | FWHM | Mn/Ni | Ni/Al | Al/O |
| 5 NA-Mn | 857.0 | 3.836 | 75.6 | 2.451 | 0.043 | 0.433 | 0.51 |
| 10 NA-Mn | 857.3 | 3.729 | 69.5 | 2.638 | 0.092 | 0.567 | 0.36 |
| 15 NA-Mn | 856.9 | 3.773 | 69.6 | 2.454 | 0.064 | 0.660 | 0.56 |
| 20 NA-Mn | 856.0 | 3.927 | 68.2 | 2.766 | 0.044 | 0.716 | 0.62 |

### 5.3.2 The catalytic activities of the Ni/Al$_2$O$_3$ catalysts with various percent loading of nickel in carbon dioxide hydrogenation

The overall activities of the 0.5 wt% Mn modified on Ni/Al$_2$O$_3$ catalysts with various percent loading of nickel (5, 10, 15, 20 wt% Ni) which were prepared by solid-state reaction were studied in $CO_2$ hydrogenation reaction. Firstly, using 0.1 g catalyst packed in the quartz microreactor The total gas flow rate was 21.2 ml/min with the $H_2/CO_2$ ratio of 10/1. Secondly, the catalysts were reduced in flowing $H_2$ at 400°C for 4 h. Finally, the reaction was carried out at 500°C and 1 atm total pressure.

The conversion and product selectivity during carbon dioxide hydrogenation reaction are exhibited in Table 5.17. The steady state of $CO_2$ hydrogenation of the 0.5 wt% Mn modified on Ni catalysts were ranging between 50.9-66.1% in the order: 20 NA-Mn > 15 NA-Mn > 10 NA-Mn > 5 NA-Mn. It was found that increasing the amount of nickel loading resulted in higher $CO_2$ conversion. The 20 wt% Ni modified

catalysts prepared by solid-state reaction showed the highest $CO_2$ conversion at 66.1%. According to $H_2$ chemisorption, the amount of nickel active sites of 20 NA-Mn catalysts were the highest the Ni active sites. Further the 20 wt% nickel catalysts promoted with manganese showed a shift of the reduction temperature towards lower temperature so, the reduction of NiO was easier than among all catalysts. Moreover 20 wt% nickel catalysts showed the highest $H_2$ consumption. That is the NiO particles can be higher reduced. However, BET surface area of 20 NA-Mn catalysts exhibited lower than 5 NA-Mn but according to XPS analyses, the nickel particles obtained from 20 NA-Mn were higher located on the external surface of alumina than 5 NA-Mn. It is suggested that the nickel species may not be well spread on support during solid state reaction. Therefore, the BET surface area of 5 NA-Mn catalysts possibly exhibited only the surface area of support.

Table 5.17  The conversion, and product selectivity during $CO_2$ hydrogenation at initial and steady-state conditions of nickel catalysts with various percent loading of nickel after calcination at 500 °C

| Sample | Conversion [a] (%) | | Product selectivity [a] (%) | | | |
|---|---|---|---|---|---|---|
| | Initial [b] | Steady state [c] | Initial [b] | | Steady state [c] | |
| | | | CH₄ | CO | CH₄ | CO |
| 5 NA-Mn | 58.1 | 50.9 | 100 | 0 | 100 | 0 |
| 10 NA-Mn | 59.5 | 51.3 | 100 | 0 | 100 | 0 |
| 15 NA-Mn | 66.7 | 63.9 | 100 | 0 | 100 | 0 |
| 20 NA-Mn | 65.3 | 66.1 | 100 | 0 | 100 | 0 |

[a] $CO_2$ hydrogenation was carried out at 500 °C, 1 atm, $H_2/CO_2$ = 10.

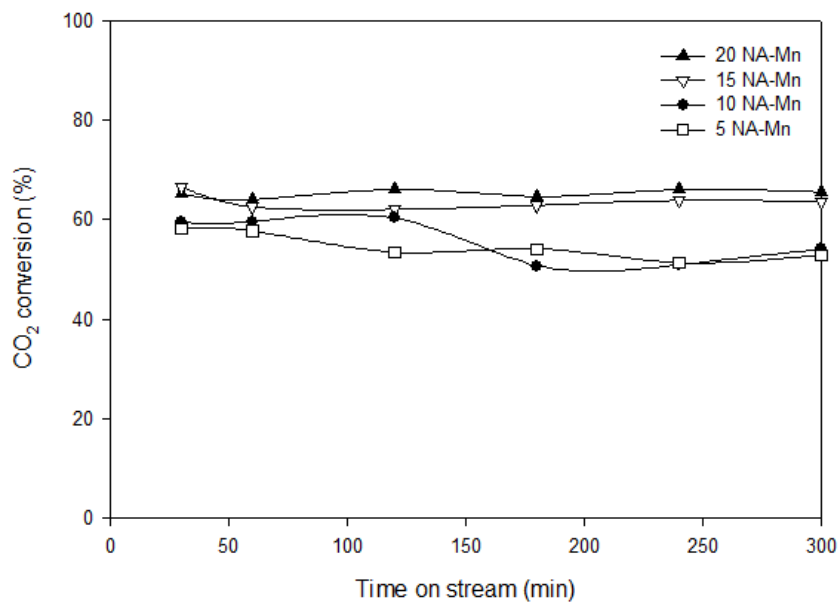[b] After 30 min of reaction.

[c] After 4 h of reaction.



Figure 5.12  Carbon dioxide conversion of 0.5 wt% Mn modified on nickel catalysts with various percent loading of Ni

**5.4 Effect of the preparation methods between solid-state reaction and incipient wetness impregnation**

**5.4.1 The catalytic activities of the Ni/Al$_2$O$_3$ catalysts prepared between solid-state reaction and incipient wetness impregnation method in carbon dioxide hydrogenation**

The label used for the catalysts are as shown:

**X-Mn-Y-NA** is referred to the catalyst prepared by solid-state reaction which a mixture of gibbsite, and the percent loading of manganese acetate and nickel nitrate.

**X-Mn-Y-NA-Imp** is referred to the catalyst prepared by incipient wetness impregnation which a mixture of gibbsite calcined at 500°C., and the percent loading of manganese acetate and nickel nitrate.

**X-Mn-Y-NA-Imp-seq** is referred to the catalyst prepared by incipient wetness impregnation which a mixture of gibbsite calcined at 500°C., and the percent loading of nickel nitrate and then impregnated manganese acetate later.

The overall activities of the Ni/Al$_2$O$_3$ catalysts with various percent loading of manganese and nickel which were prepared by solid-state reaction and incipient wetness impregnation were studied in CO$_2$ hydrogenation reaction.

The conversion and product selectivity during carbon dioxide hydrogenation reaction are shown in Table 5.18. The steady state of CO$_2$ hydrogenation of the Ni-based catalysts were ranging between 22.6-66.1%. It was found that the non-modified nickel catalysts of 5 and 20 wt% loading of nickel prepared by either the solid-state reaction or the incipient wetness impregnation method, the one prepared by incipient wetness impregnation showed the higher CO$_2$ conversion than the solid-state reaction. According to H$_2$ chemisorption, the amount of nickel active sites of nickel-based catalysts prepared by the incipient wetness impregnation were higher

(results in part 1). Moreover the smaller NiO crystallite size found in the XRD patterns of the nickel catalysts prepared by incipient wetness impregnation so the smaller NiO may be easier to reduce to active nickel particles.

Comparing the 0.5 wt% Mn modified on nickel catalysts of 5 and 20 wt% loading of nickel prepared by either the solid-state reaction or the incipient wetness impregnation method, the catalysts prepared by solid-state reaction of both 5 and 20 wt% loading of nickel showed higher $CO_2$ conversion than prepared by the incipient wetness impregnation method. Although the modified nickel catalysts obtained from incipient wetness impregnation method showed higher the amount of nickel active sites from $H_2$ chemisorption (result in part 1). but BET surface area and the average pore volume of the modified nickel catalysts obtained from incipient wetness impregnation were lower than the ones obtained from solid-state reaction (result in part 1). It is suggested that the nickel particles may block some pores of alumina support therefore so that in the pore volume decreased upon nickel loading. The location of nickel particles may influence the $CO_2$ reactant and active nickel particles [20].

Comparing the non-modified nickel catalysts of 5 and 20 wt% loading of nickel prepared by either the solid-state reaction or the incipient wetness impregnation method, both the 5 wt% loading of nickel catalyst prepared by the solid-state reaction and the incipient wetness impregnation showed lower $CO_2$ conversion. According to $H_2$-TPR technique, the 5 wt% nickel catalysts showed a shift of the reduction temperature towards higher temperature so, the reduction of NiO was harder (result in part 3). Further the amounts of nickel active sites of 5 wt% nickel catalysts from $H_2$ chemisorption were lower than 20 wt% nickel catalysts. Therefore the amounts of Ni active sites may affect this reaction.

Comparing the 0.5 wt% Mn modified nickel catalysts of 5 and 20 wt% loading of nickel prepared by either the solid-state reaction or the incipient wetness impregnation method, both the 20 wt% loading of modified-Ni catalyst prepared by the solid-state reaction and the incipient wetness impregnation showed higher $CO_2$ conversion. According to $H_2$-TPR technique, the 20 wt% modified nickel catalysts showed a shift of the reduction temperature towards lower temperature so, the reduction of NiO was easier (result in part 3). Moreover, the amounts of nickel active sites of 20 wt% modified nickel catalysts from $H_2$ chemisorption were higher than 5 wt% modified nickel catalysts.

Comparing the 0.5 wt% Mn modified on 5 wt% nickel catalysts prepared by either the solid-state reaction, the incipient wetness impregnation method or the sequence loading of manganese and nickel in the incipient wetness impregnation method. It was found that the 0.5 wt% Mn modified on 5 wt% nickel catalysts prepared by the solid-state reaction exhibited the highest $CO_2$ conversion at 51.3%. It is suggested that the modified nickel catalysts obtained from the incipient wetness impregnation had smaller NiO crystallite size which may be easier to reduce to active nickel particles. However, the smaller NiO crystallite size may block some pores of alumina support so that the pore volume and BET surface area decreased (result in part 1). According to $H_2$ chemisorption, the amount of nickel active sites of modified nickel catalysts were lower. Moreover the sequence loading of manganese and nickel in the incipient wetness impregnation showed the lowest $CO_2$ conversion at 22.6%. Therefore the sequence loading might influence this reaction.

62

**Table 5.18** The conversion, and product selectivity during $CO_2$ hydrogenation at initial and steady-state conditions of nickel catalysts after calcination at 500 °C

| Sample | Conversion [a] (%) | | Product selectivity [a] (%) | | | |
|---|---|---|---|---|---|---|
| | | | Initial [b] | | Steady state [c] | |
| | Initial [b] | Steady state [c] | CH₄ | CO | CH₄ | CO |
| 5 NA | 25.6 | 26.4 | 100 | 0 | 100 | 0 |
| 5 NA-Imp | 21.5 | 26.5 | 100 | 0 | 100 | 0 |
| 0.5 Mn-5 NA | 58.1 | 51.3 | 100 | 0 | 100 | 0 |
| 0.5 Mn-5 NA-Imp | 42.2 | 42.1 | 100 | 0 | 100 | 0 |
| 0.5 Mn-5 NA-Imp-seq | 37.1 | 22.6 | 100 | 0 | 100 | 0 |
| 20 NA | 34.5 | 32.3 | 8.3 | 91.7 | 4.8 | 95.2 |
| 20 NA-Imp | 44.7 | 37.5 | 5.5 | 94.5 | 4.8 | 95.2 |
| 0.5 Mn-20 NA | 65.3 | 66.1 | 100 | 0 | 100 | 0 |
| 0.5 Mn-20 NA-Imp | 63.3 | 62.9 | 100 | 0 | 100 | 0 |

[a] $CO_2$ hydrogenation was carried out at 500 °C, 1 atm, $H_2/CO_2 = 10$.

[b] After 30 min of reaction.

[c] After 4 h of reaction

CHAPTER 6

CONCLUSIONS AND RECOMMENDATIONS

6.1 Conclusions

In the present work, the effects of various promoters on the properties of $Ni/Al_2O_3$ catalyst obtained by the solid- state reaction using the mixture of nickel nitrate, gibbsite, and promoters were investigated. For comparison purposes, the catalysts were prepared by the incipient wetness impregnation method. The catalytic activities were tested in carbon dioxide hydrogenation. The results can be concluded as followed:

1) When prepared by the solid-state reaction, the $Ni/Al_2O_3$ catalysts with Mn and Cu promoters exhibited higher $CO_2$ conversion than the non-modified catalysts. The nickel catalysts promoted with Mn exhibited higher $CO_2$ hydrogenation activity than the catalysts promoted with Cu. The better catalytic activity was explained by the higher dispersion of nickel particles on the surface of support and a shift of the reduction temperature towards lower temperature, therefore, the reduction of NiO was easier. However, the catalysts prepared with various amounts of manganese loading between 0.5-2 wt% Mn exhibited similar $CO_2$ conversion during the 5 h time-on-stream.

2) The non-modified nickel catalysts prepared by the incipient wetness impregnation showed higher $CO_2$ conversion than the ones prepared by solid-state reaction. It can be explained by the higher amount of nickel active sites and the smaller NiO crystallite size obtained from the impregnation method. However, when modified with Mn the modified nickel catalysts prepared by the solid-state reaction

showed the higher $CO_2$ conversion than the incipient wetness impregnation due to improved Ni dispersion and reducibility.

## 6.2 Recommendations

1) Temperature has a major effect in the reaction of carbon dioxide hydrogenation. Therefore, it is interesting to investigate the different temperatures in reaction which would affect the catalytic performance.

2) The location of metal on support influences the catalytic activity so it is interesting to investigate the location of metal on alumina using TEM technique.

3) The copper and manganese promoters may be reduced with hydrogen during reduction step so it is interesting to study the ability in reduction of copper and manganese oxide using $H_2$-TPR technique.

REFERENCES

1. Zhang, T.A. *How to recuperate industrial waste heat beyond tire and space* 2013 2009, April 6; Available from: http : //vcharkarn.com/vnews/152208

2. Kiehl, J.T., Kevin, E.T. , *Bulletin of the American Meteorological Society*. Earth's annual global mean energy budget. . Vol. 78. 1997. 197-208.

3. Li, F., Yu, X., Pan, H., Wang, M., and Xin, X. , *Synthesis of $MO_2$ (M = Si, Ce, Sn) nanoparticles by solid-state reactions at ambient temperature.* Solid State Sciences 2000. **2**: p. 767-772.

4. Hezhi, L., Xiujing, Z., Xueguang, W., Xionggang, L., Weizhong, D., *Effect of $CeO_2$ addition on $Ni/Al_2O_3$ catalysts for methanation of carbon dioxide with hydrogen.* Journal of Natural Gas Chemistry 2012. **21**: p. 703-707.

5. Narcis, H., Jamil, T., Pilar, R., *Catalytic Processes for Activation of $CO_2$.* Catalonia Institute for Energy Research. 2013, Spain.

6. Anthony, R.W., *Synthesis Methods*. Basic Solid State Chemistry. 1999, New York Wiley Press. p.407.

7. Chakrabarty, D.K., *Solid state reactions.* Soild state chemistry. 1996, India: New Age International Limited. p.115.

8. Aivin, B.S., *Alumina*. Catalyst Supports and Supported Catalysts. 1909, United States of America Butterworths.

9. Santos, S.P., Santos, S.H., and Toledo, S.P. , *Standard transition aluminas. Electron microscopy studies.* Materials Research 2000. **3**(4): p. 104-114.

10. Carnes, M. *Nickel*. 2013, November 1; Available from: http : //en.wikipedia.org/w/index.php?title=Nickel&oldid=579753982

11. Anmin, Z., Weiyong, Y., Haitao, Z., Hongfang, M., and Dingye, F, *$Ni/Al_2O_3$ catalysts for syngas methanation: Effect of Mn promoter.* Journal of Natural Gas Chemistry, 2012. **21**: p. 170-177.

12. Yan, L., Dazhuang, L., *Study of bimetallic Cu-Ni/$\gamma$-$Al_2O_3$ catalysts for carbon dioxide hydrogenation.* International Journal of Hydrogen Energy 1999. **24**: p. 351-354.

13. Robert, W.D., Dennis, R.H., Frederick, W.W., Heather, D.W., *$C_2$-$C_{5+}$ olefin production from $CO_2$ hydrogenation using ceria modified Fe/Mn/K catalysts* Catalysis Communications 2011. **15**: p. 88-92.

14. Srisawat, J., *Characteristics and catalytic properties of alumina-silica bimodal pore supported cobalt catalyst for carbon monoxide hydrogenation*, in *Chemical Engineering Faculty of Engineering* 2007, Chulalongkorn University.

15. Chitpong, N., *Characteristics and catalytic properties of boron-modified zirconia-supported cobalt catalyst for carbon monoxide hydrogenation*, in *Chemical Engineering Faculty of Engineering* 2007, Chulalongkorn University.

16. Sung, C.L., and others, *Promotion of hydrocarbon selectivity in $CO_2$hydrogenation by Ru component.* Journal of Molecular Catalysis A: Chemical 2004. **210**: p. 131-141.

17. Taochaiyaphum, N., *Characteristics and catalytic properties of glycothermal-derived zirconia supported cobalt catalysts in carbonmonoxide hydrogenation*, in *Chemical Engineering Faculty of Engineering* 2004, Chulalongkorn University.

18. Natpakan, S., *Preparation of $Co/Al_2O_3$ catalysts by solid-state reaction between gibbsite and various cobalt precursors*, in *Chemical Engineering Faculty of Engineering*. 2010, Chulalongkorn University.

19. Titiporn, S.a.J., P. *The effects of Mn and Cu promoters on the properties of $Ni/Al_2O_3$ catalysts prepared by solid-state reaction.* in *TIChE Conference 2013*. 17-18 October 2013. Thailand.

20. Zhang, Y., Jacobs, G., Sparks, E. D., Dry, E.M., and Davis, H.B., *CO and $CO_2$ hydrogenation study on supported cobalt Fischer-Tropsch synthesis catalysts* Catalysis Today, 2002. **71**: p. 411-418.

21. Zhang, H., Dong, Y., Fang, W., Lian, Y, *Effects of composite oxide supports on catalytic performance of Ni-based catalysts for CO methanation.* Chinese Journal of catalysis, 2013. **34**: p. 330-335.

22. Izabela, C., Francois, L., Fabio, R., Jorg, W., Serge, B., Alexander, W., *Characterization of surface processes at the Ni-based catalyst during the methanation of biomass-derived synthesis gas: X-ray photoelectron spectroscopy (XPS).* Applied Catalysis A: General 2007. **329**: p. 68-78.

APPENDIX

APPENDIX A

CALCULATION FOR CATALYST PREPARATION

**1. Preparation of modified Ni/Al$_2$O$_3$ catalysts by Mn and Cu by solid-state reaction**

Preparation of modified Ni/Al$_2$O$_3$ catalysts by solid-state reaction between gibbsite, nickel nitrate and different promoters (manganese acetate and copper nitrate) are shown as follows:

- Preparation of the mechanical mixture of gibbsite (Al(OH)$_3$), nickel nitrate (Ni(NO$_3$)$_2$.6H$_2$O, and manganese acetate ((C$_2$H$_3$O$_2$)$_2$Mn.4H$_2$O) with percent loading of 20 wt% Ni and 1 wt% Mn are shown as follows:

**Reagent:**    - Gibbsite (Al(OH)$_3$)

Molecular weight    =    78 g/mol

- Nickel (II) nitrate hexahydrate (Ni(NO$_3$)$_2$.6H$_2$O)

Molecular weight    =    290.79 g/mol

- Manganese (II) acetate tetrahydrate ((C$_2$H$_3$O$_2$)$_2$Mn.4H$_2$O)

Molecular weight    =    245.09 g/mol

**Calculation:** For percent loading of 20 wt% Ni and 1 wt% Mn are shown as follows:

Based on 2 g of modified Ni/Al$_2$O$_3$ catalysts:

| | |
|---|---|
| 100 g modified Ni/Al$_2$O$_3$ catalysts | consisted of nickel equal to 20 g Ni |
| 2 g modified Ni/Al$_2$O$_3$ catalysts | consisted of nickel equal to 0.4 g Ni |
| 100 g modified Ni/Al$_2$O$_3$ catalysts | consisted of manganese equal to 1 g Mn |
| 2 g modified Ni/Al$_2$O$_3$ catalysts | consisted of manganese equal to 0.02 gMn |
| 100 g modified Ni/Al$_2$O$_3$ catalysts | consisted of alumina equal to 79 g Al$_2$O$_3$ |
| 2 g modified Ni/Al$_2$O$_3$ catalysts | consisted of alumina equal to 1.58 g Al$_2$O$_3$ |

The amount of nickel required 0.4 g was prepared from the nickel precursor as (Ni(NO$_3$)$_2$.6H$_2$O) which had the molecular weight of 290.79 g/mol, and the molecular weight of Ni is 58.693 g/mol. Therefore, the amount of nickel precursor required as (Ni(NO$_3$)$_2$.6H$_2$O) can be calculated as follows:

$$\text{(Ni(NO}_3)_2.6H_2O) \text{ required} = \frac{\text{(MW of (Ni(NO}_3)_2.6H_2O) \times \text{(Nickel required)}}{\text{(MW of Ni)}}$$

$$= \frac{(290.79 \text{ g/mol}) \times (0.4 \text{ g Ni})}{(58.693 \text{ g Ni/mol})}$$

$$= 1.9818 \text{ g of (Ni(NO}_3)_2.6H_2O)$$

The amount of manganese required 0.02 g was prepared from the manganese precursor as $((C_2H_3O_2)_2Mn.4H_2O)$ which had the molecular weight of 245.09 g/mol, and the molecular weight of Mn is 54.938 g/mol. Therefore, the amount of manganese precursor required as $((C_2H_3O_2)_2Mn.4H_2O)$ can be calculated as follows:

$$((C_2H_3O_2)_2Mn.4H_2O) \text{ required} = \frac{(MW \text{ of } ((C_2H_3O_2)_2Mn.4H_2O)) \times (Mn \text{ required})}{(MW \text{ of } Mn)}$$

$$= \frac{(245.09 \text{ g/mol}) \times (0.02 \text{ g Mn})}{(54.938 \text{ g Mn/mol})}$$

$$= 0.08922 \text{ g of } ((C_2H_3O_2)_2Mn.4H_2O)$$

Alumina 1.58 g consisted of aluminium equal to:

$$\text{Aluminium} = \frac{1.58 \text{ g } Al_2O_3}{} \left| \frac{1 \text{ mol } Al_2O_3}{101.961 \text{ g } Al_2O_3} \right| \frac{2 \text{ mol } Al}{1 \text{ mol } Al_2O_3} \left| \frac{26.982 \text{ g } Al}{1 \text{ mol } Al} \right.$$

$$= 0.8362 \text{ g Al}$$

The amount of aluminium required 0.8362 g was prepared from the gibbsite as $(Al(OH)_3)$ which had the molecular weight of 78 g/mol, and the molecular weight of Al is 26.982 g/mol. Therefore, the amount of gibbsite required as $(Al(OH)_3)$ can be calculated as follows:

$$\text{(Al(OH)}_3\text{) required} = \frac{\text{(MW of (Al(OH)}_3\text{))} \times \text{(Al required)}}{\text{(MW of Al)}}$$

$$= \frac{\text{(78 g/mol)} \times \text{(0.8362 g Al)}}{\text{(26.982 g Al/mol)}}$$

$$= \quad 2.4174 \text{ g of (Al(OH)}_3\text{)}$$

In the same manner to prepare modified $Ni/Al_2O_3$ catalysts which were used the other of promoter such as copper nitrate. The molecular weight of promoter is as follows:

- Copper (II) nitrate $(Cu(NO_3)_2.2.5H_2O)$

Molecular weight $\quad = \quad$ 232.59 g/mol

## 2. Preparation of modified $Ni/Al_2O_3$ catalysts by Mn by incipient wetness impregnation

For percent loading of 20 wt% Ni and 1 wt% Mn supported on $Al_2O_3$ using incipient wetness impregnation are shown as follows:

Based on 2 g of modified $Ni/Al_2O_3$ catalysts:

100 g modified Ni/Al$_2$O$_3$ catalysts     consisted of nickel equal to 20 g Ni

2 g modified Ni/Al$_2$O$_3$ catalysts     consisted of nickel equal to 0.4 g Ni

100 g modified Ni/Al$_2$O$_3$ catalysts     consisted of manganese equal to 1 g Mn

2 g modified Ni/Al$_2$O$_3$ catalysts     consisted of manganese equal to 0.02 gMn

100 g modified Ni/Al$_2$O$_3$ catalysts     consisted of alumina equal to 79 g Al$_2$O$_3$

2 g modified Ni/Al$_2$O$_3$ catalysts     consisted of alumina equal to 1.58 g Al$_2$O$_3$

For using 1.58 g of Al$_2$O$_3$;

The amount of nickel required 0.4 g was prepared from the nickel precursor as (Ni(NO$_3$)$_2$.6H$_2$O) which had the molecular weight of 290.79 g/mol, and the molecular weight of Ni is 58.693 g/mol. Therefore, the amount of nickel precursor required as (Ni(NO$_3$)$_2$.6H$_2$O) can be calculated as follows:

$$\text{(Ni(NO}_3)_2.6\text{H}_2\text{O) required} = \frac{\text{(MW of (Ni(NO}_3)_2.6\text{H}_2\text{O)} \times \text{(Nickel required)}}{\text{(MW of Ni)}}$$

$$= \frac{(290.79 \text{ g/mol}) \times (0.4 \text{ g Ni})}{(58.693 \text{ g Ni/mol})}$$

$$= 1.9818 \text{ g of (Ni(NO}_3)_2.6\text{H}_2\text{O)}$$

The amount of manganese required 0.02 g was prepared from the manganese precursor as $((C_2H_3O_2)_2Mn.4H_2O)$ which had the molecular weight of 245.09 g/mol, and the molecular weight of Mn is 54.938 g/mol. Therefore, the amount of manganese precursor required as $((C_2H_3O_2)_2Mn.4H_2O)$ can be calculated as follows:

$$((C_2H_3O_2)_2Mn.4H_2O) \text{ required} = \frac{(MW \text{ of } ((C_2H_3O_2)_2Mn.4H_2O)) \times (Mn \text{ required})}{(MW \text{ of Mn})}$$

$$= \frac{(245.09 \text{ g/mol}) \times (0.02 \text{ g Mn})}{(54.938 \text{ g Mn/mol})}$$

$$= 0.08922 \text{ g of } ((C_2H_3O_2)_2Mn.4H_2O)$$

## APPENDIX B

## CALCULATION OF THE CRYSTALLITE SIZE

**Calculation of the crystallite size by Scherrer equation**

The crystallite size was calculated from the half-height width of the diffraction peak of XRD pattern using the Debye-Scherrer equation.

From Scherrer equation:

$$D = \frac{K\lambda}{\beta \cos\theta} \tag{i}$$

Where    D   =   Crystallite size, Å

       $K$   =   Crystallite-shape factor = 0.9

       $\lambda$   =   X-ray wavelength, 1.54056 Å for CuK$_\alpha$

       $\theta$   =   Observed peak angle, degree

       $\beta$   =   X-ray diffraction broadening, radian

The X-ray diffraction broadening ($\beta$) is the pure width of a powder diffraction free of all broadening due to the experiment equipment. Standard $\alpha$-alumina is used to observe the instrumental broadening since its crystallite size is larger than 2000 Å. The X-ray diffraction broadening ($\beta$) can be obtained by using Warren's formula.

From Warren's formula:

$$\beta^2 = \beta^2_M - \beta^2_S \tag{ii}$$

$$\beta \quad = \quad \sqrt{\beta_M^2 - \beta_S^2}$$

Where    $\beta_M$   =   The measured peak width in radians at half peak height

        $\beta_S$   =   The corresponding width of a standard material

**Example**: Calculation of the crystallite size of NiO on $Al_2O_3$ support

The half-height width of peak   =   $0.3905^{\circ}$ (from Figure B.1)

                               =   $0.3905 \times 0.0174$

                               =   $0.006812$ radian

The corresponding half-height width of peak of $\alpha$-alumina   =   $0.000785$ radian

The pure width               =   $\sqrt{\beta_M^2 - \beta_S^2}$

                               =   $\sqrt{0.006812^2 - 0.000785^2}$

                               =   $0.006766$ radian

$\beta$      =     $0.006766$ radian

$2\theta$     =     $43.24^{\circ}$

$\theta$      =     $21.62^{\circ}$    =    $0.3772$ radian

$\lambda$      =     $1.54056$ Å

The crystallite size    =    $\dfrac{0.9 \times 1.54056}{(0.006766) \cos 0.3772}$

                               =    $220.40$ Å
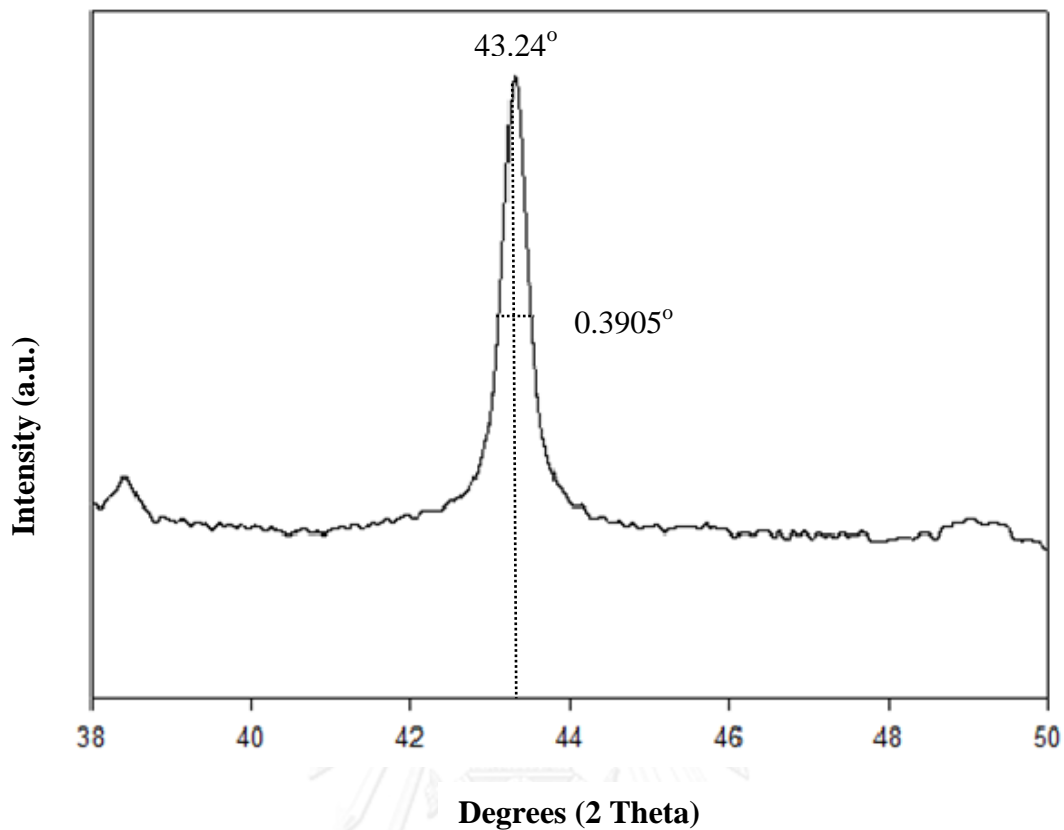
                               =    $22.0$ nm

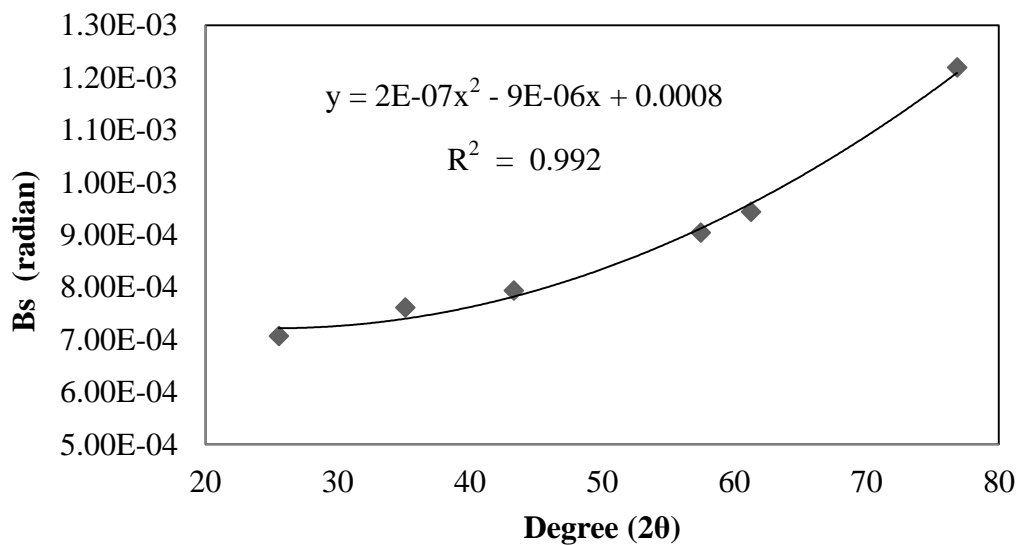Figure B.1  The measured peak of Ni/Al$_2$O$_3$ to calculate the crystallite size



Figure B.2  The plot indicating the value of line broadening due to the equipment

# APPENDIX C

## CALCULATION FOR TOTAL $H_2$ CHEMISORPTION

Calculation of the amount of active sites and the percent dispersion of metal on the surface of catalysts, which a stoichiometry of H/Ni = 1, measured by $H_2$ chemisorption is as follows:

| | | | |
|---|---|---|---|
| The weight of catalyst used | = | W | g |
| Loop volume dosed | = | $V_{loop}$ | μL |
| Integral area of $H_2$ peak after adsorption | = | $A_i$ | unit |
| Integral area of 100 μL of standard $H_2$ peak | = | $A_f$ | unit |
| Molar volume of gas at STP ($V_g$) | = | 22414 | $cm^3$/mol |
| % Metal used | = | %M | % |
| Molecular weight of the metal | = | MW. | a.m.u. |
| Avogadro's number | = | $6.023 \times 10^{23}$ | molecules/mol |

Amount of $H_2$ adsorbed on catalyst $= \dfrac{V_{loop} \times \sum(Af - Ai)}{(W \times Af)}$ = A  μL/$g_{cat}$

Amount of $H_2$ adsorbed on catalyst    =    A/1000    = B  $cm^3$/$g_{cat}$

Mole of $H_2$ adsorbed on catalyst    =    B/$V_g$    mol/ $g_{cat}$

Molecule of $H_2$ adsorbed on catalyst   (Metal active site)

$$= 2 \times \text{mole of } H_2 \times 6.023 \times 10^{23} \text{ molecules } H_2/\text{g cat}$$

%Dispersion    =    $(S_f \times mole_{H2}/mole_{nickel}) \times 100$  %

APPENDIX D

CALIBRATION CURVES

This calibration curves are used for calculation of the composition of reactant and products in $CO_2$ hydrogenation reaction. The reactant is carbon dioxide and the main product is methane, including carbon monoxide is a by-product in $CO_2$ hydrogenation reaction.

The concentrations of gas composition in the feed and product streams were analyzed by a Shimadzu GC-8A (molecular sieve 5Å column) gas chromatograph equipped with TCD (Thermal conductivity detector).

The x-axis showed the area reported by gas chromatography and the y-axis showed the mole of reagent. The calibration curves of $CO_2$, CO, and methane are exhibited in the following figures.

Table D.1  Condition use in Shimadzu modal GC-8A

| Parameters | Condition Shimadzu GC-8A (TCD) |
|---|---|
| Width | 5 |
| Slope | 50 |
| Drift | 0 |
| Min. area | 10 |
| T.DBL | 0 |
| Stop time | 12 |
| Atten | 5 |
| Speed | 10 |
| Method | 1 |
| Format | 1 |
| SPL.WT | 100 |
| IS.WT | 1 |



$$y = 0.5405e^{2E-05x}$$

$$R^2 = 0.9956$$
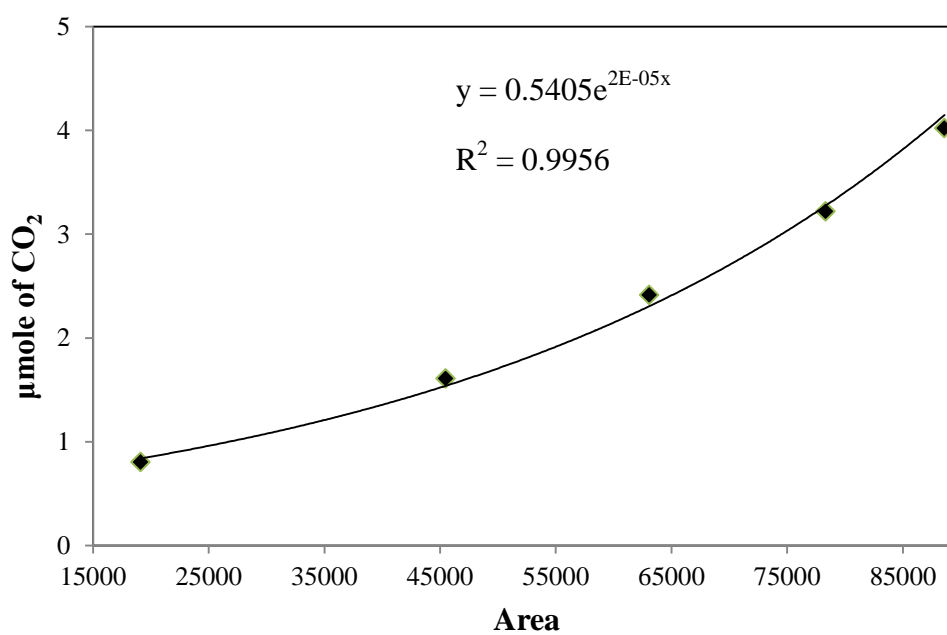
Figure D.1  The calibration curve of carbon dioxide
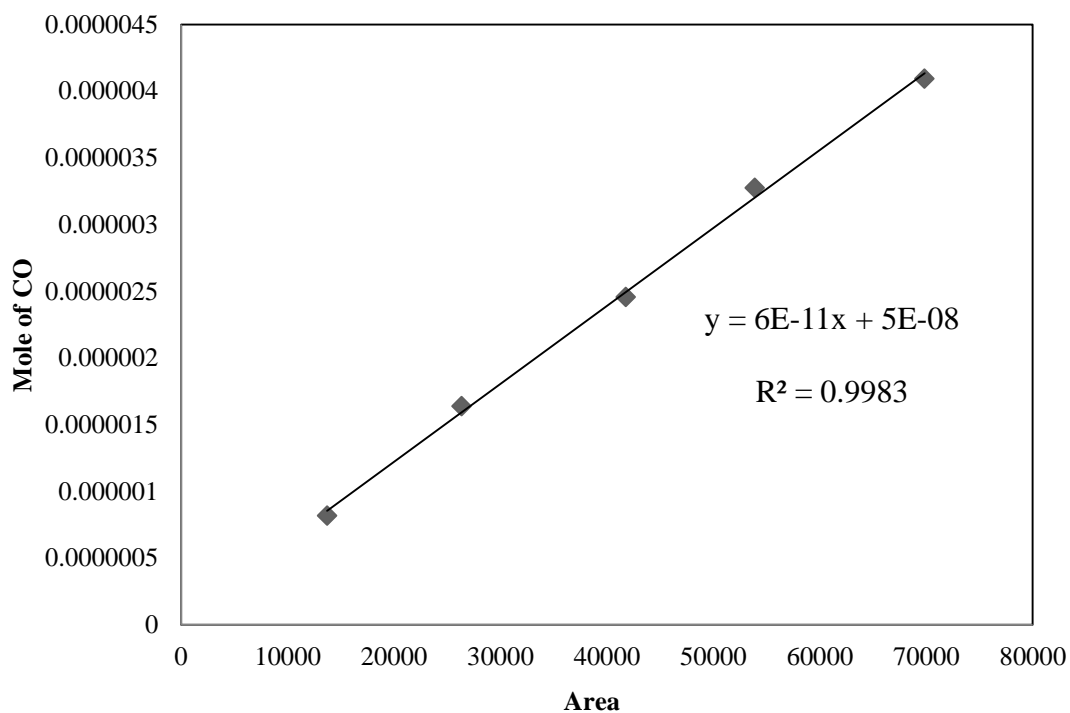
Figure D.2  The calibration curve of carbon monoxide

$y = 6E\text{-}11x + 5E\text{-}08$

$R^2 = 0.9983$
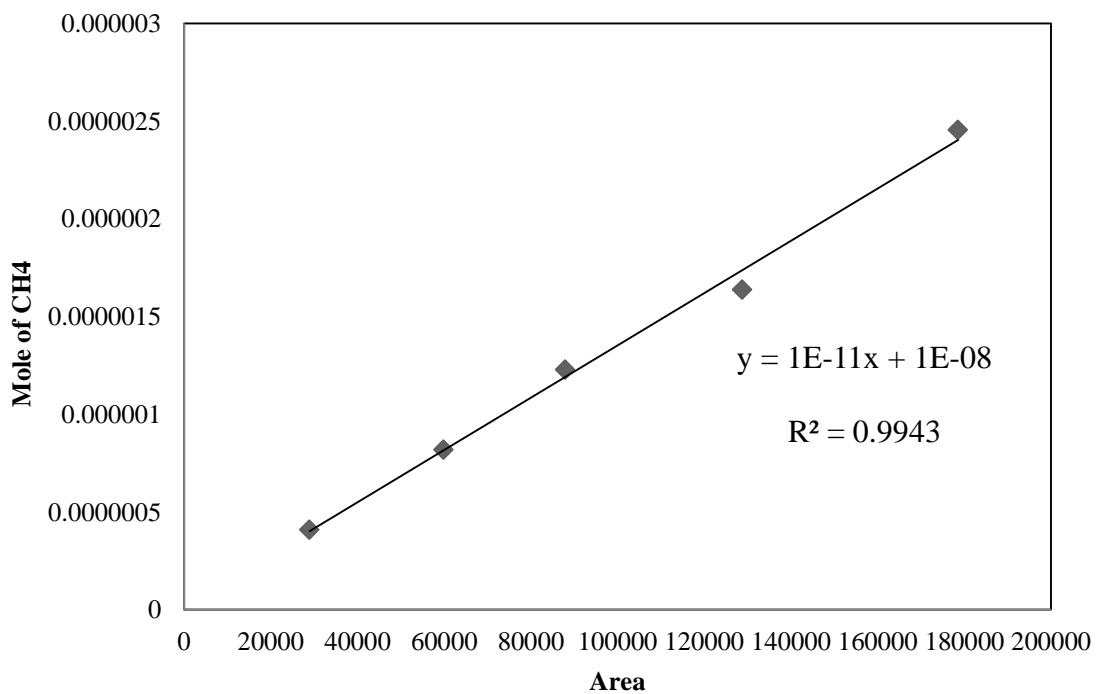


Figure D.3  The calibration curve of methane

$y = 1E\text{-}11x + 1E\text{-}08$

$R^2 = 0.9943$

# APPENDIX E
## CALCULATION OF CO$_2$ CONVERSION

The catalytic activity for the CO$_2$ hydrogenation was calculated in terms of activity for CO$_2$ conversion.

Carbon dioxide conversion is defined as moles of carbon dioxide converted with respect to carbon dioxide in feed as follows:

$$CO_2 \text{ conversion (\%)} = \frac{(\text{mole of } CO_2 \text{ in feed} - \text{mole of } CO_2 \text{ in product}) \times 100}{(\text{mole of } CO_2 \text{ in feed})}$$

# VITA

Miss Titiporn Sae-lim was born on 12th November 1989, in Bangkok, Thailand. She graduated in Bachelor degree of Chemical Technology from Chulalongkorn University, Thailand in May 2012. Since May 2012, she has been studying in Master degree of Chemical Engineering from Chulalongkorn University.

List of publication:

Titiporn Sae-lim, and Joongjai Panpranot, "The effects of Mn and Cu promoters on the properties of Ni/Al2O3 catalysts prepared by solid-state reaction", Proceedings of the 23rd TIChE Conference, Khon Kaen, Thailand, Oct.17-18, 2013.